

Zeitschrift: IABSE reports = Rapports AIPC = IVBH Berichte
Band: 76 (1997)
Rubrik: Theme D: Site measurement

Nutzungsbedingungen

Die ETH-Bibliothek ist die Anbieterin der digitalisierten Zeitschriften auf E-Periodica. Sie besitzt keine Urheberrechte an den Zeitschriften und ist nicht verantwortlich für deren Inhalte. Die Rechte liegen in der Regel bei den Herausgebern beziehungsweise den externen Rechteinhabern. Das Veröffentlichen von Bildern in Print- und Online-Publikationen sowie auf Social Media-Kanälen oder Webseiten ist nur mit vorheriger Genehmigung der Rechteinhaber erlaubt. [Mehr erfahren](#)

Conditions d'utilisation

L'ETH Library est le fournisseur des revues numérisées. Elle ne détient aucun droit d'auteur sur les revues et n'est pas responsable de leur contenu. En règle générale, les droits sont détenus par les éditeurs ou les détenteurs de droits externes. La reproduction d'images dans des publications imprimées ou en ligne ainsi que sur des canaux de médias sociaux ou des sites web n'est autorisée qu'avec l'accord préalable des détenteurs des droits. [En savoir plus](#)

Terms of use

The ETH Library is the provider of the digitised journals. It does not own any copyrights to the journals and is not responsible for their content. The rights usually lie with the publishers or the external rights holders. Publishing images in print and online publications, as well as on social media channels or websites, is only permitted with the prior consent of the rights holders. [Find out more](#)

Download PDF: 08.08.2025

ETH-Bibliothek Zürich, E-Periodica, <https://www.e-periodica.ch>



Theme D

Site Measurement

Leere Seite
Blank page
Page vide

Verification of Capacity by Proof Loading

Andrzej S. NOWAK

Professor

University of Michigan

Ann Arbor, MI, USA

Andrzej S. Nowak received his PhD from Warsaw University of Technology, Poland, and has been at University of Michigan since 1979. He has been involved in reliability-based development of the LRFD bridge design codes in the United States and Canada. He also has an extensive experience in field testing of bridges.

Vijay K. SARAF

Doctoral Student

University of Michigan

Ann Arbor, MI, USA

Vijay K. Saraf is a doctoral student at the University of Michigan. The topic of his dissertation is the development of reliability-based criteria for proof load testing of bridges.

Summary

The objective of the paper is to demonstrate an efficient proof load testing procedure for existing bridges. Proof load level required for meaningful tests is approximately twice the legal load. In the State of Michigan, the legal 11-axle truck can weigh over 70 tons. In this study, military tanks were used. Each M-60 tank weighs about 55 tons over the length of about 4.5 m (15 ft). The structural performance was measured in terms of stress/strain level and deflection. Any nonlinearity of response was considered as an indication of inadequate strength. The measured stress levels were unexpectedly low. This can be justified by unintended composite action, effect of non-structural components such as parapets, and more uniform distribution of load.

1. Introduction

The objective of the study was to verify the load carrying capacity of an existing steel girder bridge. The load capacity of the bridge was in question due to extensive corrosion of steel girders. Initial rating showed that the bridge had marginal operating rating factor for the 11-axle two-unit truck (77 tons), which is the heaviest vehicle allowed in Michigan. To avoid the load limit posting, it was decided to verify if the bridge is safe to carry the normal truck traffic by using a proof load test. The bridge was instrumented and proof load was applied in form of two military M-60 tanks. The paper describes the test methodology and the results.

2. Selected bridge

The bridge is a simply supported steel girder bridge carrying state route M-50 over Grand River in Jackson County, Michigan. The total span length is 14.6 m. The total width is 13.8 m. It carries one lane in each direction with total ADT of 11,900. As shown in Fig. 1, there are ten steel girders, a 165 mm thick reinforced concrete slab, and a 170 mm thick bituminous overlay. It was designed to behave as non-composite section. Based on the initial inspection, lower flanges of steel girders were found heavily corroded. At some locations close to mid-span, the flange thickness was reduced by as much as 60 percent. This reduces the moment capacity of steel girder by about 25 percent. There was not much corrosion in steel girders near the supports, and reinforced concrete slab was in moderate condition.

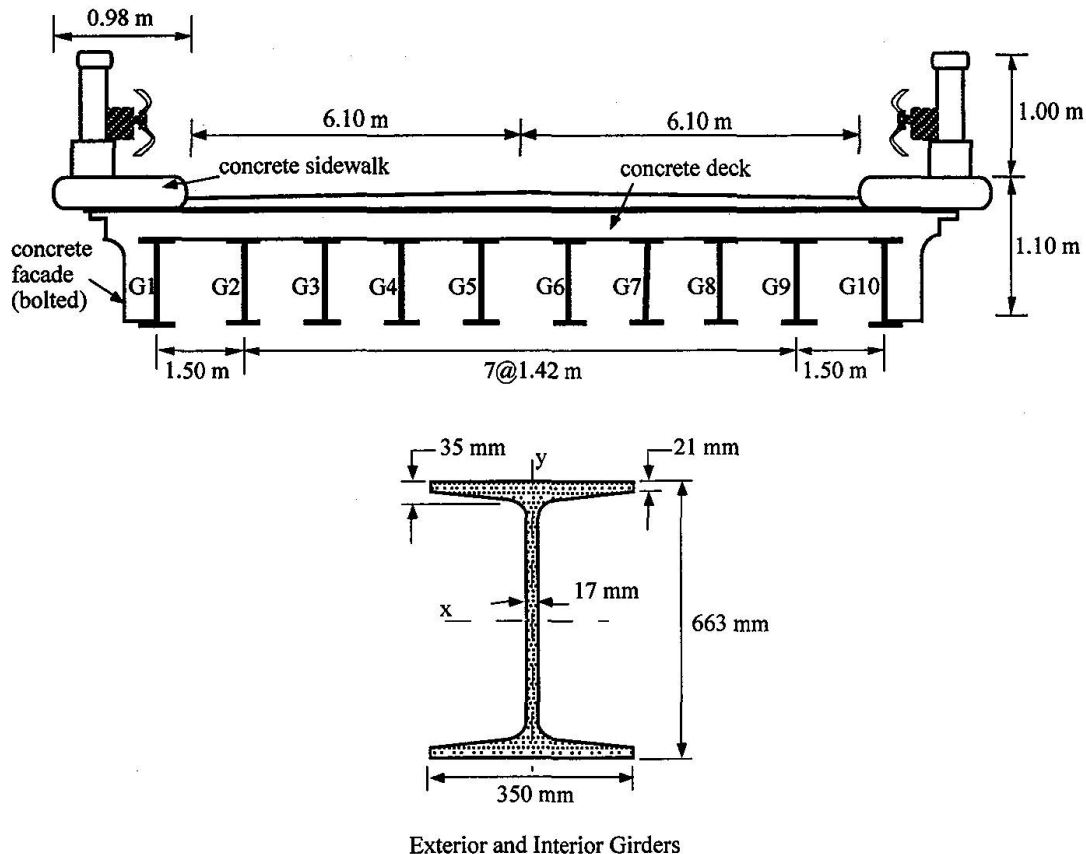


Fig. 1 Cross-section of the tested bridge

3. Analysis of the bridge

Based on the specifications in the Michigan Bridge Analysis Guide, the remaining capacity to carry live load and impact corresponding to the operating rating was determined to be 1,550 kNm per lane. In preliminary calculations, the inventory rating factors were 0.98 and 0.53 for H15 and HS20 trucks, respectively [1]. The operating rating factor for the 11-axle two-unit truck was 0.95. A rating factor less than 1.0 indicates that the bridge is deficient. The critical limit state for this bridge was the moment capacity at mid-span. The shear capacity was found to be adequate at all sections. These rating factors were reduced after the site inspection to include better estimates of the steel section loss. The revised inventory rating factor was 0.60 for H15 truck and operating rating factor was 0.45 for the 11-axle truck.

Since proof load testing requires careful comparison of analytical and experimental results during the testing in order to avoid accidental overload, two different types of analytical models were prepared by using the semi-continuum method developed by Jaeger and Bakht [3]. In the first model, the structural properties were taken as specified in design drawings, i.e., the slab-girder-interaction was considered to be non-composite and the effect of non-structural components was not included. For second model, the possibility of unintended composite action and contribution of non-structural members, such as parapets and railings, etc., were incorporated. For both models the supports were idealized as pin supports.

For the proof load test, a heavy load is used to test the bridge. The load is increased in several steps until the yield capacity of the bridge, or a pre-specified load limit is reached. Usually, the yield capacity of a bridge is very high. Therefore, this bridge was loaded only up to a predetermined load limit. Since, the objective of the test is to check if the bridge can carry the maximum allowable load, the applied proof load should exceed the legal load by a comfortable margin of safety. If the target proof load is successfully reached without any distress, then the resulting operating factor would be 1.0.

4. Selection of proof load

The target proof load was calculated using the draft report on NCHRP project no. 12-28(13) A, by multiplying the maximum legal load by a factor of safety of 1.4. It was further multiplied by an impact factor. According to the AASHTO Specifications [1], the impact factor would be 1.29. However, for this bridge, it was taken to be 1.10, because the dynamic experiments conducted by Nassif and Nowak [7] showed that the multi-axle vehicles with heavy loads exhibit much smaller impact. Also, it was decided to load one lane at a time. Therefore, the target load was increased by 15 percent to account for unloaded adjacent lanes.

The required proof load was calculated to be an 11-axle two-unit truck with gross vehicle weight of 1,210 kN. In previous studies by other researchers [4], concrete barrier blocks were placed on a flat bed truck to load the bridge. Each block weighs about 22 kN. Therefore, for this study the required number of blocks would be so large that it would not be possible to safely fit all of them on one truck. Therefore, a different scheme had to be prepared. Since the moment capacity at mid-span was found to be critical in preliminary calculations, it was decided to apply a load that would cause the equivalent proof load moment.

The innovative idea was to use M-60 military tanks on flat-bed trailers to achieve a very high target proof load level. The side view of the M-60 tank is shown in Fig. 2. Each tank weighs over 490 kN. This load is distributed over a small track of 4.5 m. Two such tanks were required to test this bridge. These tanks were provided by the Michigan National Guard. Only the four rear axles of each trailer were used to load the bridge. Each tank was placed on a flat bed trailer, such that the load on rear tandem axles was maximum. Both tanks had the same total weight. However, the configuration of the trailers was different. Therefore, the resulting axle loads were different.

For first load step, the tank on military trailer was placed close to support, to start with small mid-span moment. Then, the mid-span moment was increased gradually in several steps by moving the trailer towards mid-span. For third load case, the trailer was placed so that it caused maximum mid-span moment. For the fourth load case, the second trailer was positioned on the bridge, to further increase the moment. Load was also moved to three different transverse load positions. They were called upstream, center and downstream, depending on their location with respect to the flow of the river underneath, i.e. in upstream load position the trailers were placed close to the upstream railing.

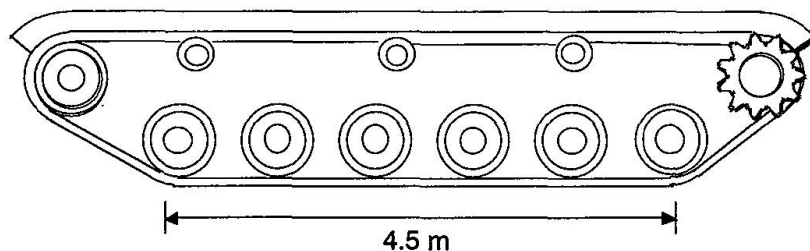


Fig. 2 Side view of M-60 tank



5. Instrumentation

Results of the test were closely monitored for any sign of distress. Several strain transducers were placed on steel girders close to mid-span and quarter-points. These transducers are reusable and clamped to the lower flanges of girders. Deflections at mid-point of all interior girders were measured using LVDT's. Deflections at quarter-points of selected girders were also measured. After placing the trailers in each load position, the data from each instrument was collected using a portable data acquisition system. The real time response of selected transducers was also monitored at all stages of testing. The data from LVDT's and strain transducers was collected by a portable SCXI-1200 data acquisition system. The system consists of a four slot SCXI-1000 chassis, one SCXI-1200 data acquisition card and two SCXI-1100 multiplexers. Each multiplexer can handle up to 32 channels of input data. The current system is capable of handling 64 channels of strain or deflection inputs. Up to 32 additional channels can be added if required. A portable field computer is used to store, process and display the data on site. A typical data acquisition setup is shown in Figure 3.

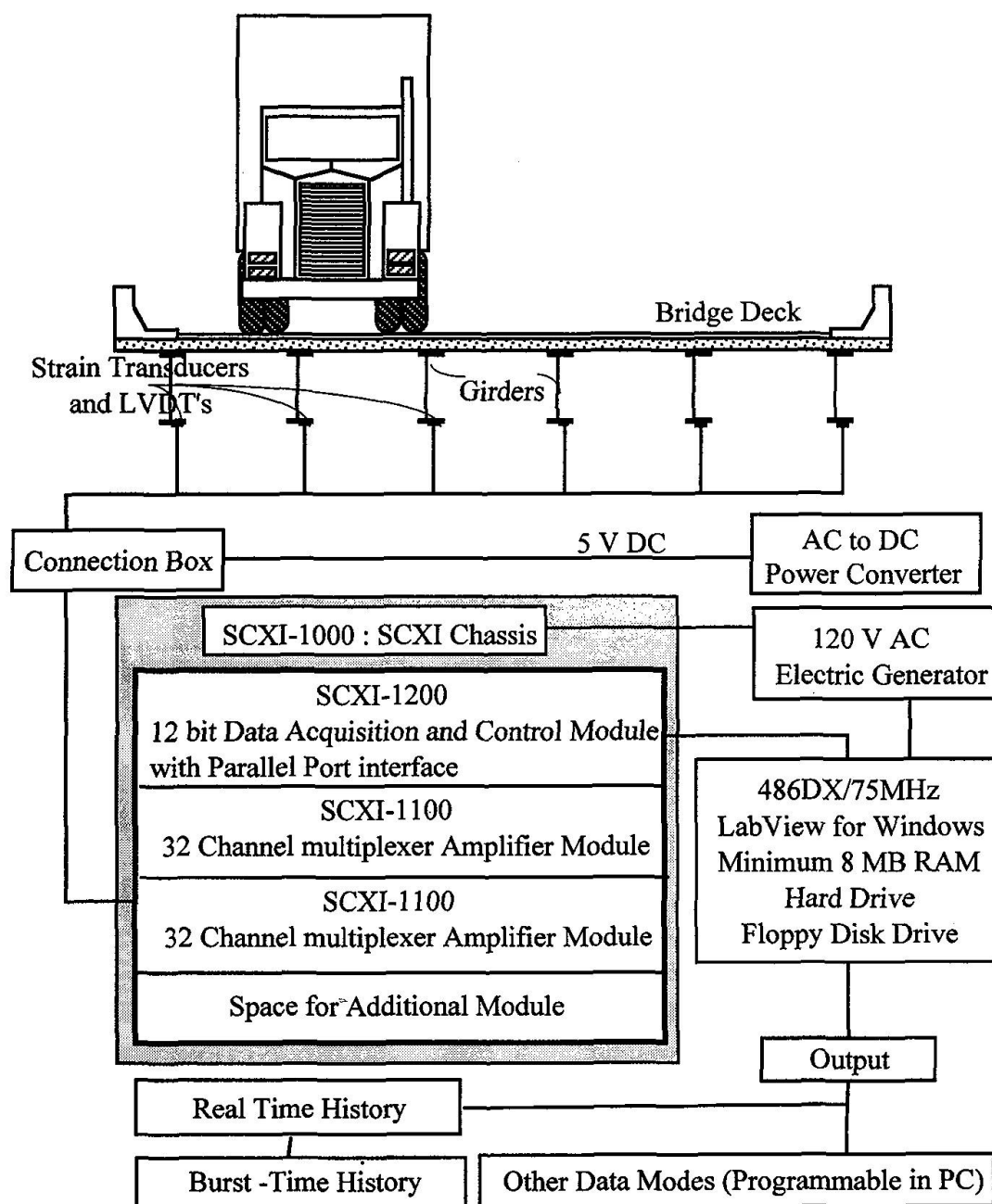


Fig. 3 SCXI Data Acquisition System Setup.

6. Proof load test results

During the test a maximum mid-span moment of 2,120 kNm was applied, which is over 2.6 times the moment caused by the HS20 design truck. The target proof load level was successfully reached without any noticeable distress. Therefore, the operating rating factor for an 11-axle two-unit truck is 1.0, after the test. Figs. 4 to 6 show the stresses at mid-span of girders for downstream, center and upstream loading, respectively. The four points in these figures relate to the four test load cases described in Section 4.

The maximum stress of 19.4 MPa was observed during experiments, for girder no. 3. It is less than 0.1 of the yield strength of steel. Also, for all girders, the stress increased linearly with increasing lane moment, and similar behavior was observed for center and upstream load cases. This indicates the extra safety reserve in the structure. The predicted maximum analytical stresses were 29 MPa and 48 MPa for composite and non-composite models, respectively. It shows that the composite action between concrete slab and steel girders is present even at loads several times larger than the design load. The non-structural members also contributed to the overall flexural strength of the structure. Lateral distributions of girder deflections at mid-span are shown in Figs. 7 to 9. Although several diaphragms were severely deteriorated, the actual load sharing between girders is more uniform than analytically predicted. Following the test, the bridge was opened for normal traffic without any load posting.

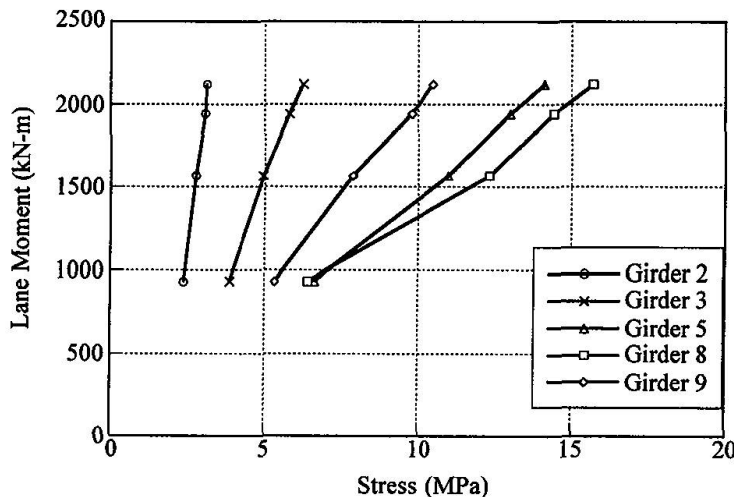


Fig. 4 Stresses at mid-span of girders for downstream loading

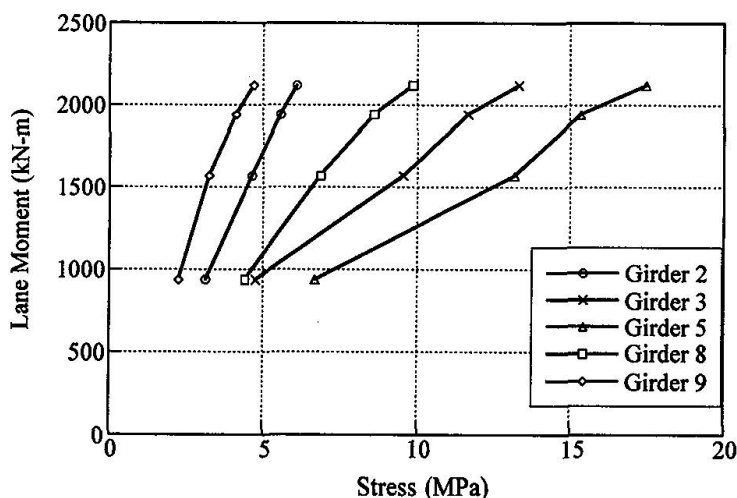


Fig. 5 Stresses at mid-span of girders for center loading

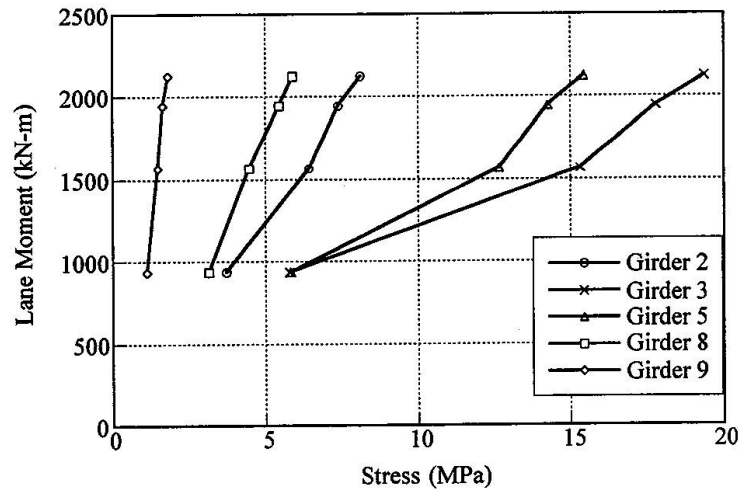


Fig. 6 Stresses at mid-span of girders for upstream loading

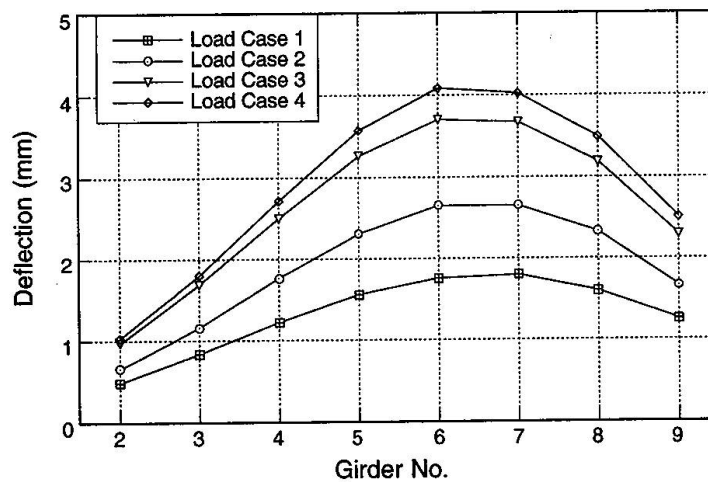


Fig. 7 Lateral distribution of deflections at mid-span for downstream loading

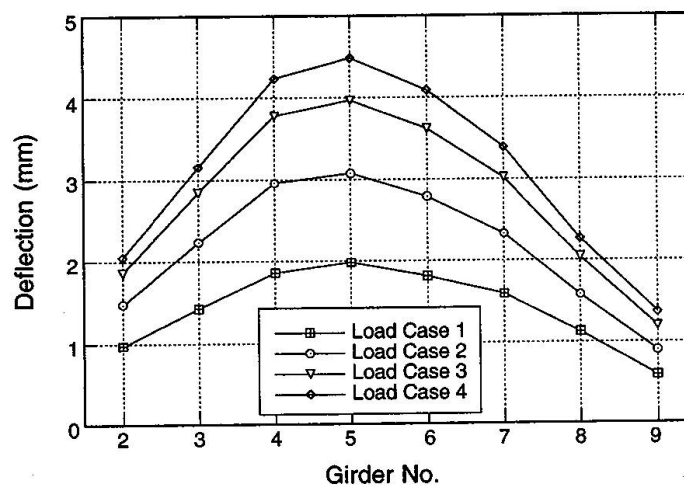


Fig. 8 Lateral distribution of deflections at mid-span for center loading

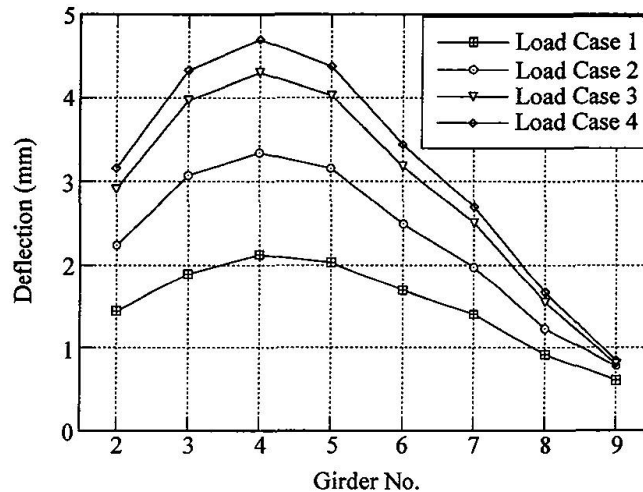


Fig. 9 Lateral distribution of deflections at mid-span for upstream loading

7. Conclusions

The proof load tests can be used as an efficient method to verify the minimum load carrying capacity of the structure. It may require a relatively greater effort, but it provides immediate answers about the load carrying capacity. The proof load must be considerably larger than legal load.

As a result of proof load test described in this paper, the bridge was found to be safe to operate under normal traffic.

Acknowledgments

The research presented in this paper has been partially sponsored by the Michigan Department of Transportation, the Great Lakes Center for Truck Transit Research, National Science Foundation, IDEA Transportation Research Board, NATO Collaborative Research Grants, and the University of Michigan, which is gratefully acknowledged.

References

1. AASHTO Standard Specifications for Bridge Design, American Association of State Highway and Transportation Officials, Washington, DC, 1992.
2. Hwang, E-S. and Nowak, A.S., "Simulation of Dynamic Load for Bridges," ASCE Journal of Structural Engineering, Vol. 117, No. 5, May 1991, pp. 1413-1434.
3. Jaeger, L.G., and B. Bakht, *Bridge Analysis by Microcomputer*. McGraw-Hill Book Company, New York, 1989.
4. Juntunen, D.A., and M.C. Isola, *Proof Load Test of R01 of 61131 M-37 over CSX Railroad*, South of Bailey. Michigan. Michigan Department of Transportation. Lansing, MI, April 1995.
5. Lichtenstein, A. G. *Bridge Rating Through Nondestructive Load Testing*. NCHRP report no. 12-28(13) A, June 1993.
6. *Michigan Bridge Analysis Guide*. Michigan Department of Transportation, Lansing, MI, December 1983.
7. Nassif, H. and Nowak, A.S., 1995, "Dynamic Load Spectra for Girder Bridges", Transportation Research Record, No. 1476, pp. 69-83.

Leere Seite
Blank page
Page vide

Measurements on Railway Bridges to Determine Axle Loads and Stress Range Spectra

Leopold SCHWARZ

Professor
Technical University
Vienna, Austria



Leopold Schwarz, born 1932, received his degree in Civil Engineering and doctoral degree from the University of Vienna. In 1980 he founded a department of experimental research in the field of steel construction. He acts as an expert on steel structures.

Summary

The construction monitoring system presented in this article is designed for the construction of railway bridges. When monitoring bridge structures, it is the task to permanently record the type, intensity, position, duration and frequency of the impact loads as well as the resulting effects on the whole system like elongations, vibrations etc. and the condition of construction components such as supports, expansion joints etc. Moreover, the experimental determination of the stress-time history in an assessment point makes it possible to determine the exact traffic load factor for the fatigue assessment of the supporting structure.

1. Introduction

Environment, structure and function of a construction are too be understood as components of a system. All factors within this system undergo changes over the time thus mainly causing the ageing process of the construction. One of the problems even the first bridges were confronted with is the constant growth of heavy traffic. In practice, railway bridge dimensioning is based on the simple Load Model UIC-71 according to UIC leaflet 702 V [1] which covers the impact of usual traffic and on the basis of the Load Model SW which is equivalent to the unitised train of the load class SW/2 according to UIC leaflet 776-1E [2].

Many tests showed that stresses in various bridge components under traffic load were usually smaller than stresses due to loading assumptions. Thus, it is not economical to base the calculations of the fatigue limit on the extremely large stresses under the design load of 2×10^6 load cycles for example. For the fatigue assessment the vertical traffic load of rail vehicles is represented by a combination of various types of trains. The fatigue assessment for „usual traffic“ is carried out with mixed traffic, the fatigue assessment for „traffic with 250 kN-axles“ is carried out with heavy goods traffic. Each type of „combined traffic“ is based on the annual traffic load of 25×10^6 tons transported per track. The fatigue assessment is to be based on a life span of 100 years.

In „DRAFT ENV 1993-2 [3]: Chapter 9, April 1996“, it is proposed to use a simplified method of fatigue assessment. In the following only the assessment of the uniaxial stress will be discussed, the superimposed stress resulting from the principal- and secondary load-act will not be taken into account, either.

The assessment is defined as follows:

$$\gamma_{Ff} \Delta \sigma_{E2} \leq \Delta \sigma_c / \gamma_{Mf}$$

Notation:

γ_{Ff} is the partial safety factor for the fatigue loads, in case no other detail is given γ_{Ff} is assumed to be 1,0.

γ_{Mf} is the partial safety factor for the fatigue strength.



$\Delta\sigma_{e, \dots}$ is the reference value of the fatigue strength at 2 million stress cycles (for longitudinal stresses).

$\Delta\sigma_{E2, \dots}$ is the equivalent constant amplitude stress range (for longitudinal stresses) for 2 million stress cycles.

$$\Delta\sigma_{E2} = \lambda \Phi_2 \Delta\sigma_{71}$$

λ, \dots is the damage equivalence factor for railway bridges.

$$\lambda = \lambda_1 \cdot \lambda_2 \cdot \lambda_3 \cdot \lambda_4$$

λ_1, \dots is the "real" traffic load factor, it takes into account the length of the influence area for various types of girders. The calculation is based upon the reference construction, i.e. the moment stress of a single-span girder (σ) in the mid-span for various lengths L due to UIC mixed traffic on a single-track structure. The line load is 25 million tons per year with a fatigue life of 100 years.

λ_2, \dots is the factor taking into account the deviation from the traffic volume.

λ_3, \dots is the factor taking into account the deviation from the design life.

λ_4, \dots is the factor, which is used, if a structural element is stressed by more than one loaded track. In order to calculate the maximum stress range, two tracks are to be loaded unfavourably with the norm load train.

Φ_2, \dots is the dynamic factor (as explained in ENV 1991-3, paragraph 6.4).

$\Delta\sigma_{71, \dots} [\max\sigma_{71} - \min\sigma_{71}] \rightarrow$ The reference stress range $\Delta\sigma_{71}$ of the vertical traffic load due to Load Model UIC-71 (UIC-leaflet 702V). In order to obtain the highest and the lowest values of the stress range in a stress cycle, the load train has to be put into the position which is most unfavourable for the monitored structural element.

In accordance with "ENV 1991-3" [4] the following traffic parameters are to be considered for the assessment of the service load:

- uniform trains with standard axle loads, axle distances, a defined number and succession of railway cars and locomotive,
- standard traffic mix.

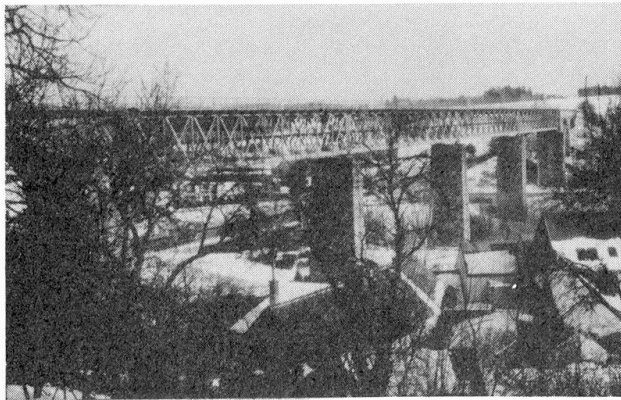


Fig. 1 Kampviadukt near Zwettl

Technical University of Vienna to determine the real axle loads of the local railway between Zwettl and Martinsberg.

The idealised mechanic model deviates from the real structural system, as it does not consider the space load-action, effective slab-width etc. accurately. Therefore the results of the statically calculated stresses for the main load-bearing construction are too large, the stresses calculated for the bracings are too small. An error of a mere 10 % due to the load-bearing model leads to an inaccuracy in the prediction of the life span of more than 30 %.

In order to obtain a realistic assessment of the stress induced on the Kamp-viaduct (Fig. 1), the "Austrian Railways" commissioned the "Department for the Experimental Research in the Fields of Steel Engineering, E 213.1", at the

2. Objectives

The "Department for Planning, Engineering-Energy" (Abt. PE-E) of the "Austrian Railways" wanted to obtain the actual wheel pressures of all goods trains and passenger trains crossing the Kamp-viaduct in Zwettl, km 21,787 (Fig. 1) over a period of two months. Further, it was the task to determine the stresses in the upper and bottom chord of the steel load-bearing structure in the first section of the bridge (Zwettl-abutment). The bridge structure consists of four discontinuous truss girders, each having an effective span of 46,64 m (Fig. 1). The system of a truss girder is 5 m high and 3,2 m wide and consists of 11 fields of the framework, each field having a web of two diagonal members.

3. Planning of the project

Two measuring areas were selected on the bridge (Fig. 2):

-) "Measuring area a" for measurements of wheel pressures and temperatures at a rail.
-) "Measuring area b", for measurements of strains and temperature at the top chord and strains at the bottom chord of a main girder.

The measuring system was designed to automatically acquire and analyse all axial stresses, strains in the chord members in the mid-span of the bridge due to traffic loads and temperatures affecting the bridge girder system over a period of two months.

The main components of such a measuring system are:

- triggering function
- acquisition of measurements provided by sensors, such as:
 - strain gauges
 - electrical resistance thermometer
 - trigger signals
- signal amplifiers
- analogue-digital converter
- an industrial computer equipped with software for acquiring, storing and analysing the measured values
- display

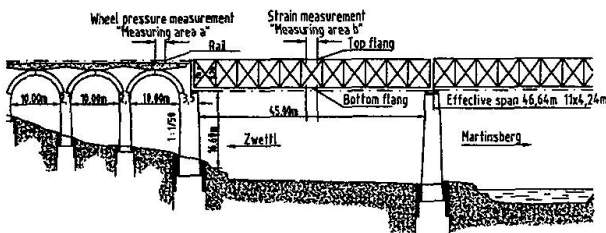


Fig. 2 The two measuring areas on the bridge structure

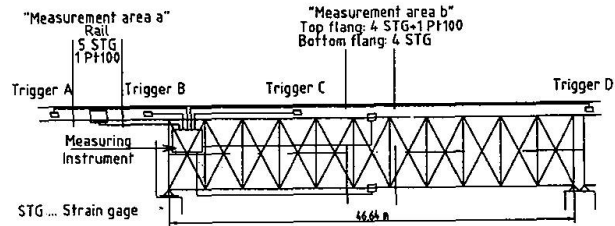


Fig. 3 Survey of the measuring points

Four triggers were located on the bridge (Fig. 3). The acquisition of measuring data was started as soon as a trigger was passed. "Measuring areas a and b" are designed to acquire data continuously during the train passage of the bridge at the speed of $v > 5 \text{ km/h}$.

The measuring system was installed on a platform between the two inspection runways in the first steel supporting structure next to the Zwettl abutment (Fig. 3). The local power supply for the measuring system was provided by the "Austrian Railways".

4. The measuring system

The measuring system was designed to monitor both

- a) the loads imposed on the supporting structure and
- b) the strains in the structural elements.

The measuring system determines the following parameters of the rail vehicles (traffic load):

- wheel pressures
- wheel distances
- speed of trains
- direction of traffic
- lateral impact
- dynamic stress
- time and date

Due to continuous strain measurements on the surface of structural members during the train passage, it is possible to calculate the

- linear states of stress (tensile, compressive and shear stresses)
- plane states of stress (principal stresses and the position of the stress ellipse).

A schematic drawing of the installed measuring system can be seen in Fig. 4.

The industrial computer controls the whole data-acquiring process. The readings are transferred on line to the hard disk and subsequently stored on a digital-audio-tape. The acquired readings are analysed and assessed either on the measuring computer or on a HP-workstation 735/125. Standard evaluations within the evaluation programme are automatised to a large extent by macros. The complete measuring equipment is installed in a 19-inch-cabinet. The power supply is secured by a 750-Watt-UPS. Fig. 3 shows the sensor locations.

A sleeper was removed in "measuring area a" for wheel-pressure measurements, the rail was instrumented with 5 strain gauges. The bending strains of the rail are used to determine the wheel load. The temperature is measured with an electrical resistance thermometer Pt 100.



“Measuring area b” was located in the mid-span of the bridge. The outer and interior upper chord of the main girder were each instrumented with two strain gauges and one electrical resistance

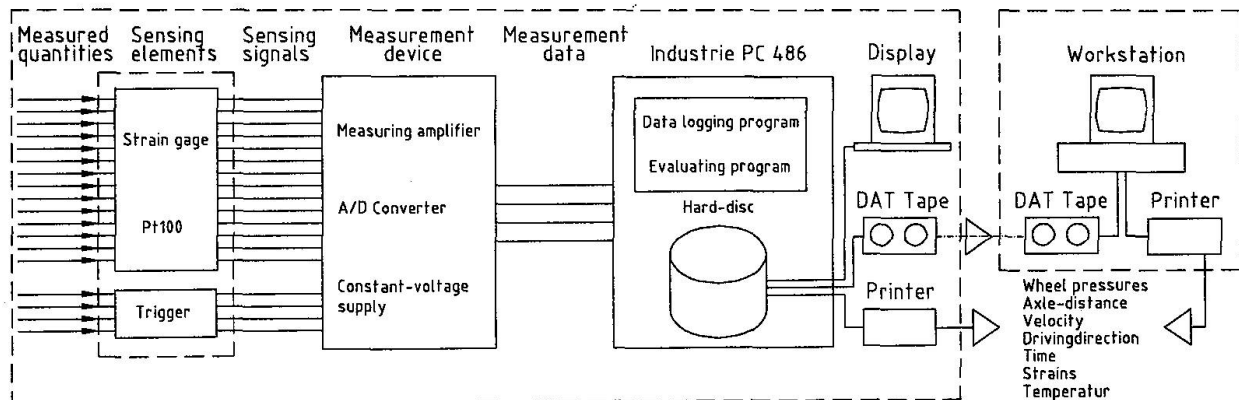


Fig. 4 Scheme of the measuring system

thermometer Pt 100. The outer and interior bottom chord of the main girder were each instrumented with two strain gauges (Fig. 7).

The measuring system is started via one of the four triggers (A, B, C or D). Trigger A and B mark the boundary of “measuring area a” and are also used for velocity measuring.

Trigger D is mounted on the rail over the first pier. As soon as a train coming from Martinsberg has arrived at the first section of the bridge, the measuring system is started by trigger D.

Trigger C registers any shunting traffic on the bridge (Fig. 3).

5. Measuring Results

The installation of the measuring system on the Kamp viaduct was started on November 30th, 1995. All measuring data of rail vehicles crossing the Kamp viaduct from December 19th, 1995 to March 23rd, 1996 were evaluated.

5.1 Measurements in „measuring area a“

Each load train is characterised by several parameters in the evaluation protocol (Fig. 5).

| JUL 2 1996 12:39:44 zug00189 Page 1 | | | |
|-------------------------------------|-----------------|-----------------|-----------------------|
| 1 | Zug-Name | : | zug00189 |
| 2 | | | |
| 3 | Anzahl Meßwerte | : | 56484 |
| 4 | Datum | : | 12-21-1995 |
| 5 | Uhrzeit | : | 08:57:21 |
| 6 | | | |
| 7 | Rad-Druck [t] | Rad-Abstand [m] | Geschwindigkeit [m/s] |
| 8 | | | |
| 9 | 8.707 | 5.835 | 5.030 |
| 10 | 9.088 | 2.566 | |
| 11 | 9.023 | 5.659 | |
| 12 | 7.446 | 2.591 | |
| 13 | 11.918 | 4.653 | |
| 14 | 10.536 | 6.263 | |
| 15 | 11.777 | 3.848 | |
| 16 | 10.548 | 6.363 | |
| 17 | 9.775 | 3.899 | |
| 18 | 11.364 | 6.414 | |
| 19 | 10.896 | 5.232 | |
| 20 | 10.112 | 8.728 | |

Fig. 5 Evaluating protocol

Each train is characterised by the:

- name of the train
 - number of readings
 - date of measuring
 - time of measuring
- The railway vehicles are characterised by their:
- wheel pressures
 - axle distances
 - velocity

If the speed of a train is not constant during the passage of „measuring area a“, the readings of the axle distances will be inaccurate. In order to give an example for the passage of „measuring area a“ by train 189, Fig. 6 shows a worksheet stating the strain-time histories and trigger signals for determining the wheel pressures and velocity. In order to examine the accuracy of the wheel-pressure measuring, „measuring area a“ was passed 12 times with a diesel-hydraulic locomotive 2043 (70,320 t).

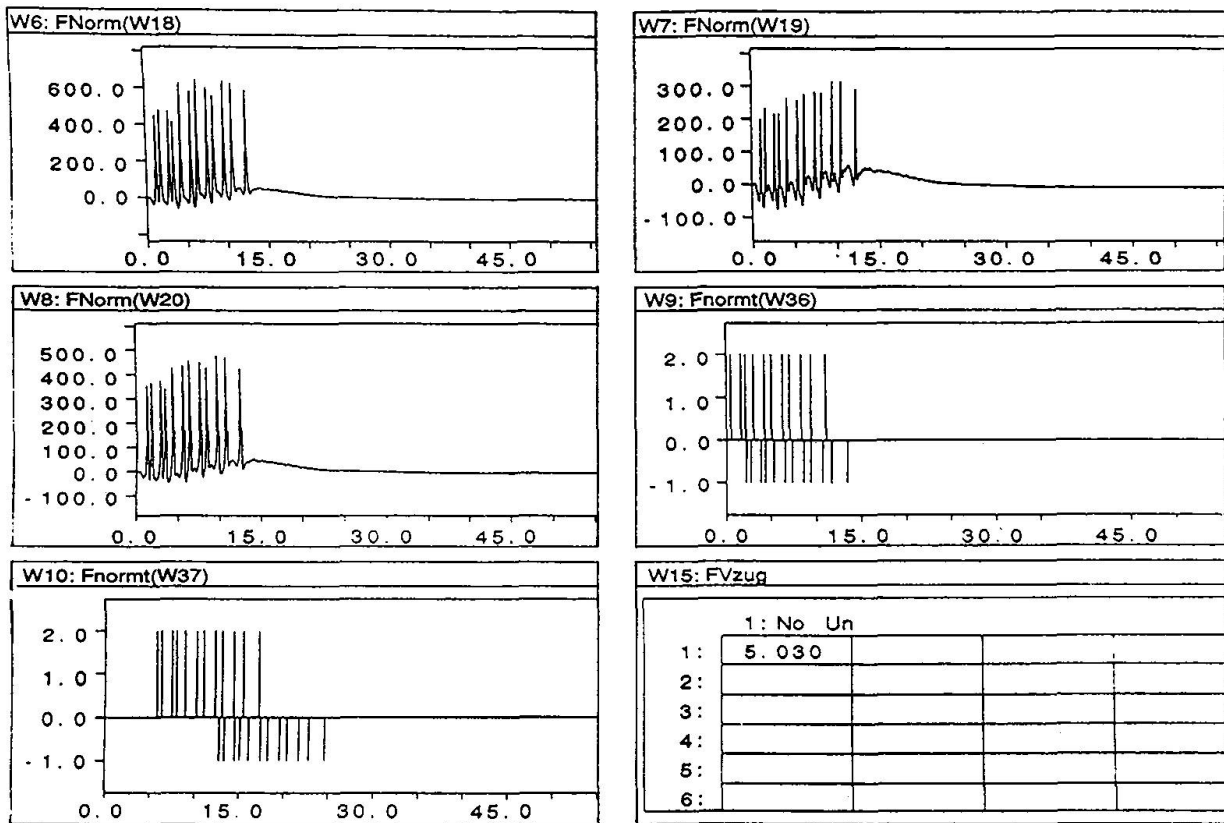


Fig. 6 Worksheet of strain-time histories and trigger-signals and velocity for the train 189 in the „measuring area a“

The evaluation of the measuring results of half of the locomotive weight (sum of four consecutive wheel loads) with regard to its accuracy shows that the mean of the 12 times measured half of the total weight X_n is:

$$X_{12} = 35,191 \text{ t}$$

the maximum deviation of the measuring value from the mean is:

$$\max \delta_i = +0,404 \text{ t} \rightarrow 1,148 \%$$

the “corrected” standard error $S_n(x)$ is: $S_{12} = \frac{s_{12}}{\sqrt{12}} = 0,071 \text{ t}$ whereby $s_{12} = 0,245 \text{ t}$

final result: $X_{12} \pm S_{12} = 35,191 \pm 0,071 \text{ t}$

the total weight of the locomotive is defined as

$$\approx 70,240 \text{ t} < X < 70,524 \text{ t}$$

5.2 Measurements in „measuring area b“

„Measuring area b“ is designed for recording the stress history of a load train which is characterised by its wheel pressures and axle distances at the upper and bottom chord (midspan of the bridge). The strain-time history at four measuring points during the passage of train 189 (time: 21.12.1995/8:57:21 h) is given as an example for the measurements at the bottom chord of the main girder. Fig. 7 gives the positions of the four strain-gauge-measuring points, Fig. 8 shows the strain-time histories on the measuring channels 9, 10, 11 and 12, respectively.

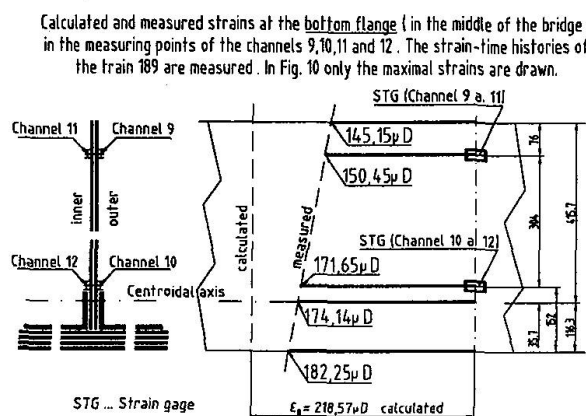


Fig. 7 Position of the four strain gauge-measuring points at the bottom flange of the main the girder

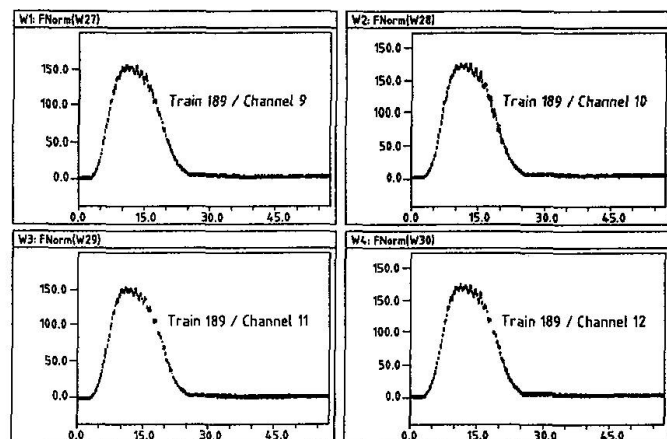


Fig. 8 Worksheet of the strain-time histories at the four strain gauge measuring points at the bottom flange during the running of the train 189

5.3 Assessment of the force imposed on the bottom chord during the passage of train 189

The measured passing time between triggers A and D indicates that the speed of the train must have diminished between both triggers thus distorting the recordings of the wheel distances (Fig. 5). In order to approximately determine the real wheel distances, a linear velocity function between trigger A and D, as shown in Fig. 9, will be assumed in the following evaluation.

V_A is the velocity of the train, measured when the head of the train comes into trigger section A-D.
 V_D is the velocity of the train, measured when the last wheel of the train leaves trigger section A-D.

This assumption allows the approximate calculation of the missing boundary condition V_D . Thus, the velocity function during the passage of section $\overline{AD} + \sum_{i=1}^{11} a_i$ (a_i is axle distance according to Fig. 5) is:

$$v(t) = V_A + \frac{V_D - V_A}{T_D - T_A} t$$

Fig. 10 explains the calculation of the corrected axle distances \bar{a}_i with the known velocity function $v(t)$.

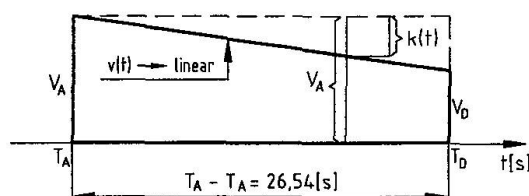
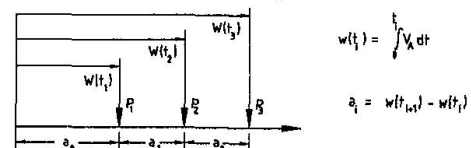


Fig. 9 Presumed linear velocity function $v(t)$ for the correction of the axle-distances a_i of train 189

Determination of axle-distance at constant velocity V_A



Determination of axle-distances at linear variable velocity $v(t)$

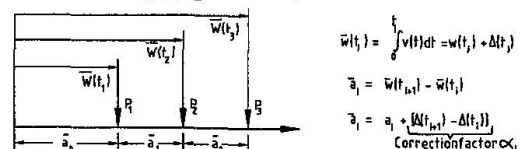


Fig. 10 Calculation of the corrected axle-distances \bar{a}_i

In Fig. 11 the goods waggon dimensions according to catalogue „Güterwagen, Daten und Details, DB 520; Ausgabe 1995“ are compared to the measured axle distances. Fig. 12 shows the determination of the maximal moment in the bridge main girder due to the wheel pressures as stated in Fig. 5 but with the corrected axle distances \bar{a}_i .

Probable succession of goods waggons of train 189 (21.12.1995/8:57:21 Time)

Characterization of probable goods waggons

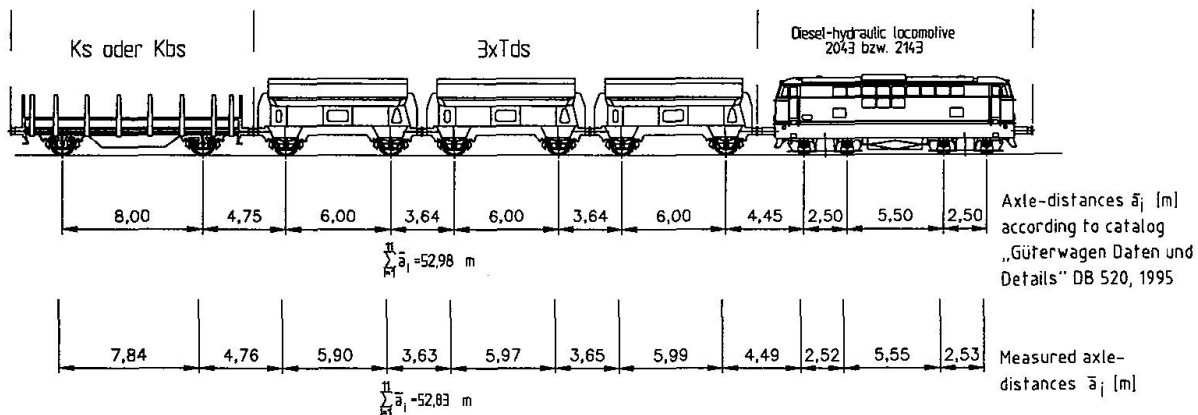


Fig.11 Checking of measured axle-distances for train 189

Fig. 12 shows the load train position causing the maximal bending moment on the mid-span of the bridge.

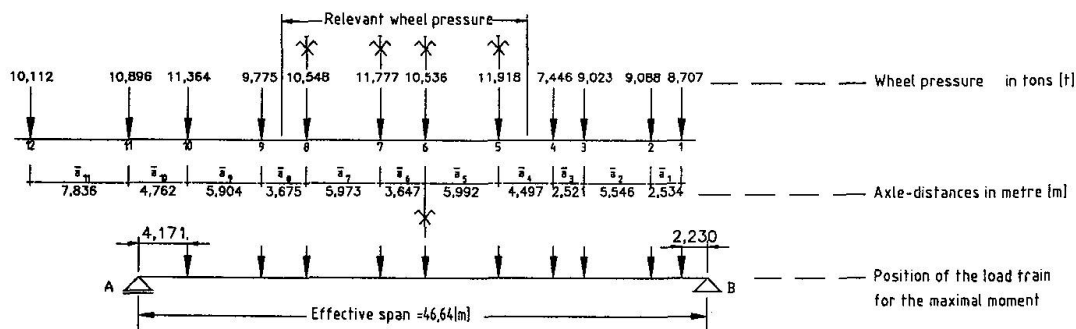


Fig.12 The position of the train 189 for maximal bending moment in the middle of the bridge

The maximum measured strains which occurred in the strain-time history during the passage of train 189 on channels 9, 10, 11 and 12, respectively, can be seen in Fig. 7. According to Fig. 7 the maximum strain in the centroidal axis of the bottom chord is $\epsilon_{Sch} = 174,13 \mu D$. This results in a normal stress of:

$$\sigma_{Sch} = 0,000174 \cdot 21000 \frac{\text{kN}}{\text{cm}^2} = 3,654 \frac{\text{kN}}{\text{cm}^2}$$

The measured normal stresses are smaller than the calculated normal stresses:

Gross sectional area:

$$\text{calculated } \sigma_G = 4,59 \frac{\text{kN}}{\text{cm}^2} > \text{measured } \sigma_{Sch} = 3,654 \frac{\text{kN}}{\text{cm}^2} \rightarrow 20,4\% \text{ smaller}$$

Net sectional area:

$$\text{calculated } \sigma_N = 5,04 \frac{\text{kN}}{\text{cm}^2} > \text{measured } \sigma_{Sch} = 3,654 \frac{\text{kN}}{\text{cm}^2} \rightarrow 27,5\% \text{ smaller}$$

The assessment of the force induced on the bottom chord during a train passage shows a difference between measured and calculated bottom chord stresses. The calculation indicates too large stresses since the mathematical model of the main girder calculation does not consider the spartial capacity of structural components like lateral bracings or roadway construction. However, due to the simplified model described above, moving loads are not taken into account when calculating bracings.



6. Comments on further data evaluation

In fatigue assessments of railway-bridges the service load is covered only by the traffic load factor λ_T . The stress in a cross-section point induced by railway vehicles is dependent on the structural system and on the position of the cross-section point in the supporting structure. For this reason, the traffic load factor is also dependent on the supporting structure and the effective span length. However, the traffic load factor λ_T is also influenced by the stress range spectrum and thus by the traffic density; fatigue life, existence of multi-track lines, combination of train types and the type of stress induced (normal or shear stress).

It is possible to determine the actual stress in an assessment point of an existing bridge with the measuring system described in chapter 4.

The further steps of the fatigue assessment are based on the hypothesis of the linear cumulative damage calculation by Palmgren-Miner.

Fatigue assessment using the damage sum:

$$D_d \leq 1 \text{ whereby } D_d = \sum \frac{n_i}{N_i}$$

n_i is the number of cycles of stress range $\Delta\sigma_i$ during the required design life.

N_i is the number of cycles of stress range $\Delta\sigma_i$ to cause failure ($\Delta\sigma_i = \text{constant}$).

Below, only the basic principles leading to the determination of traffic load factor λ_T are presented:

1. A given record of the stress-time history in one point of the supporting structure (Fig. 13 shows the stress or strain-time history in one gauge measuring point at the bottom chord).

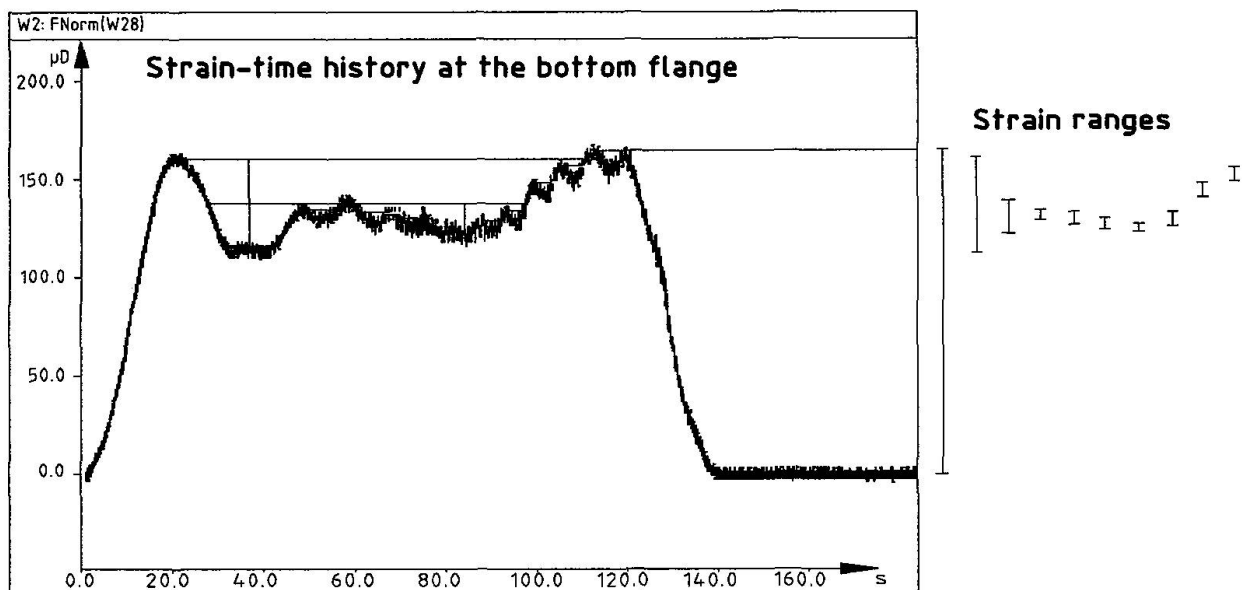


Fig. 13 Strain-time history in the measuring point at the bottom flange during the running of the train 278.

2. Stress ranges of the stress-time history are arranged in stress classes.
3. Stress ranges from the given stress-time history in the assessment point are counted-out using the "rainflow" method or "reservoir" method. The stress ranges which were recorded during the train passage are summed and arranged according to their magnitudes. They form the stress-range spectrum of the monitored train.
4. The total stress range spectrum of the train traffic is determined. The stress-range spectra of the single trains are used to determine a train total stress range spectrum related to a certain time-unit (one day in most cases).
5. Calculation of traffic load factor λ_T :

Determination of the equivalent constant amplitude stress range (for normal stresses) $\Delta\sigma_a$:

$\Delta\sigma_a$ (for a fatigue strength curve with two slopes $m_1 > m_2$) can be determined as follows:

$$\Delta\sigma_a = \left[\frac{1}{n_T} \left(\sum n_i \Delta\sigma_i^{m_1} + \Delta\sigma_D^{(m_1-m_2)} \sum n_j \Delta\sigma_j^{m_2} \right) \right]^{\frac{1}{m_1}}$$

Notation:

- $\Delta\sigma_i, \Delta\sigma_j, \dots$ The stress ranges
 $\Delta\sigma_D$ Constant amplitude fatigue limit
 m_1, m_2, \dots Constant slopes of a fatigue strength curve
 n_i, n_j, \dots Number of cycles of stress range $\Delta\sigma_i$, resp. $\Delta\sigma_j$

The equation for the traffic load factor is:

$$\lambda_T = \frac{\Delta\sigma_a}{\Delta\sigma_{UIC}}$$

$\Delta\sigma_{UIC} = \Phi \Delta\sigma_{UIC}$ Maximum stress range due to the UIC load model, multiplied by the dynamic factor Φ .

The fatigue assessment with equivalent constant amplitude stress range (normal stress) is indicated as follows:

$$\lambda_T (\gamma_{Ff} \overline{\Delta\sigma_{UIC}}) \leq \frac{\Delta\sigma_R}{\gamma_{Mf}}$$

- $\Delta\sigma_R$ Fatigue strength (normal stress) values on the fatigue strength curve for the relevant detail category, determined for the same number of stress cycles as used to calculate $\Delta\sigma_a$
 γ_{Ff} Partial safety factor for fatigue loading
 γ_{Mf} Partial safety factor for fatigue strength

7. Conclusions

The measuring system described in chapter 4 makes it possible to determine the service condition of a structural system. This monitoring concept differentiates between monitoring the load and the condition of the supporting structure. It permanently registers the position, intensity, duration, velocity and frequency of the external loads. It also records the deflections, deformations, strains, vibrations, construction settlements and changes in crack widths and temperature, it shows the condition of the supporting structure under external loads. The standard deviations of the starting parameters and the uncertainty in the calculation method according to "ENV 1993-2 DRAFT, April 1996" leads to an inexact traffic load factor λ_T . This fact speaks for the experimental determination of the stress range spectrum.

It is recommendable to solve the following tasks experimentally:

- the experimental determination of the stress-time history (stress range spectrum) in an assessment point of the supporting structure as this will lead to a more economical traffic load factor
- the determination of structural components for which the assessment of fatigue is relevant
- the determination of the plane state of stress during the train passage (temporal inconstant principle stresses and their position) in supporting structural components (gusset plate, deck plate of orthotropic plate etc.).

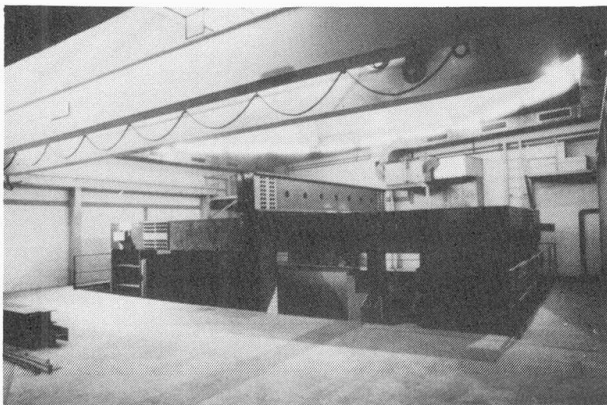


Fig. 14 Frame designed for inducing forces

The stress-time histories are also essential for the performance of service load experiments in the laboratory. By means of these tests it is possible to assess the service lives and compare the service lives of design variants. The stress-time histories, which were measured on the bridge structure and recorded on digital-audio tape, are used for the control of the testing machines. In order to conduct such experiments assessing the service loads, the author developed a frame designed for inducing forces which can be seen in Fig. 14.



8. Acknowledgements

The described measuring system was developed by the author in order to obtain accurate data of the traffic load imposed on a 90-year-old-railway bridge. The author would like to express sincere thanks to Dipl.-Ing. G. Schoitsch, head of the Dept. PE-E, Dipl.-Ing. R. Fila and Dipl.-Ing. H. Holzinger, all members of the „Austrian Railways“ head office, for their good cooperation. The author would also like to thank his collaborator Ing. P. Krajczek, especially for the time-consuming sample runs of the measuring system in order to examine the hardware and software components.

9. References

1. UIC-Merkblatt 702 V ; Lastbild für die Berechnung der Tragwerke der internationalen Strecken.
2. UIC-Merkblatt 776-1 E; Bei der Berechnung von Eisenbahnbrücken zu berücksichtigende Lasten.
3. European Prestandard, ENV 1993-2 DRAFT (April 1996) - EUROCODE 3: Design of steel structures, Part 2: Steel Bridges; European Committee for Standardization.
4. ENV 1991-3 "Eurocode 1: Basis of design and actions on structures, Part 3: Traffic loads on bridges", 1. Sept. 1995

Impact of Site Measurements on the Evaluation of Steel Railway Bridges

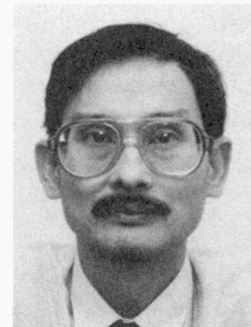
Robert A.P. SWEENEY
Assist. Chief Engineer Structures
Canadian National Railway
Montreal, PQ, Canada



George OOMMEN
System Engineer
Canadian National Railway
Montreal, PQ, Canada



Hoat LE
Bridge Testing Engineer
Canadian National Railway
Montreal, PQ, Canada



Summary

This paper provides a summary of field measured static point stresses compared to theoretical stresses, as well as measured dynamic stresses compared to theoretical stresses including impact calculated as specified in the American Railway Engineering Association (A.R.E.A.) Manual. It also proposes values for the Alpha factor and percentages of the A.R.E.A. impact values that are more adequate for the evaluation of fatigue life.

1. Introduction

In anticipation of increased axle loads, the Engineering Department of the Canadian National Railway Company (CN) has undertaken a major bridge testing program since 1988 as an adjunct to its rating program. The purpose of this program is to ensure the safety of its aging bridge plant, to prolong its life and to prioritize replacement and strengthening programs. Most of the main lines are or will be supporting 130 tonne cars (286,000 lb.) in unit trains, and 6-axle 191 tonne (420,000 lb.) locomotives.

This paper summarizes and reviews the results of 69 full scale field tests [1] of fatigue sensitive members such as bottom flanges of plate girders & stringers and bottom chords of through trusses and deck trusses. The data presented is based on maximum recorded point stresses and maximum measured impact at the maximum recorded stresses at or near the fatigue limit state.

This paper also briefly discusses whether the use of the Alpha factor and impact factor as specified in the current American Railway Engineering Association (A.R.E.A.) Manual [2] is appropriate in estimating the fatigue life of railway bridges.



2. Testing

Static and dynamic effects were measured using a pre-weighted work train under controlled conditions. Generally, the work train consisted of one or two locomotives followed by six or more cars fully loaded and sometimes followed by three empty cars. The tests were conducted at various speeds ranging from crawl speed to a maximum of 110 km/hr. (70 mph) for freight trains and 180 km/hr. (110 mph) for passenger trains. The maximum allowable speed varied depending on the zone speed of the line.

3. Selection of spans for bridge testing

The basic concept of bridge rating and safe life evaluation used by CN's Bridge department is a multiple step procedure varying from a simple check against provisions similar to those contained in Chapter 15 of the A.R.E.A. Manual [2], to a full scale load testing and crack evaluation.

The first step involves checking critical details against the design provisions of the Manual. If they are adequate, no further action is warranted.

Next, a detailed analytical evaluation is made using the approved rating and fatigue procedures. If the span and details in question pass this test, no further action is warranted.

If the previous steps reveal structural inadequacies, and the cost of replacement or repair is high compared to the cost of a successful load test, the structure is then load tested. Line importance also plays a major role in selection of bridges for testing.

4. Description of bridges and spans tested

Between 1988 and 1995, CN's Bridge department has carried out over 69 field tests. The majority of the bridges tested were on the main line supporting traffic up to 40 Million Gross Tonnes per km. (70 MGTM). Most of the traffic in Eastern Canada is of mixed type while most of the traffic in Western Canada consists of unit trains.

The tests were conducted on various types of spans, a majority of which were built around the turn of the century. Included in these tests were 28 through truss spans, 13 deck truss spans, 6 through plate girder spans and 22 deck plate girder spans.

The truss spans investigated were of riveted construction. Generally, the construction was typical of turn of the century designs. The top chords and compression members were built-up sections, while the bottom chords and other tension members were either built-up members or eye bars with or without pin plates.

All the plate girder spans were of riveted construction except one welded span, and the beam span was built using rolled I-beams.

Decks were generally open deck timber. There were three ballasted type decks. The rails were generally 68 kg/m (136 lb./3ft) continuous welded rails on heavy tonnage lines with or without "Conley" expansion joints to 57 kg/m (115 lb./3ft) jointed rails on the low tonnage lines.

The substructures consisted of stone masonry or concrete piers & abutments, steel towers and pile bents. Conditions of the bearings ranged from satisfactory to poor. In order to simulate every day field conditions, approaches were not surfaced or tamped for the tests.

5. Alpha factor

The alpha factor is defined as the ratio of the field measured static live load stress to the theoretical static live load stress. Caution should be applied when using this factor for bridge rating and predicting the remaining life, since there is no built in safe guard against unintentional errors in testing and theoretical stresses are computed according to the rating guidelines, which do not necessarily reflect true boundary conditions.

6. Discussion of the results

The field measured stresses were compared with the theoretical stresses calculations based on simple analytical models (as used in normal bridge rating practice). All of the data was taken at temperatures above the freezing point (0°C). The measured data are in the raw format without any adjustments. The measured stresses do not include dead load and are typical of the live load stress ranges that cause fatigue damage in North American railway bridges.

Figures 1, 4 and 7 show the comparison of site measured static stresses (crawl speed) under work trains to theoretical stress. Figures 2, 5 and 8 show the comparison of maximum site measured dynamic stresses to theoretical stresses with full impact as defined by A.R.E.A. chapter 15. Figures 3, 6 and 9 show the comparison of site measured dynamic stresses to theoretical stresses with modified impact values (expressed as a percentage of the theoretical impact computed as specified in the A.R.E.A. Manual). Those reduced impact values were chosen in a conservative way, such that the measured stresses are still slightly lower than the total theoretical values with only a few exceptions.

The range of loaded lengths for the members tested are shown on each of the stress comparison figures. All plotted values are the maximum values recorded and do not represent the average cross-sectional stresses nor are the effects of bending, torsion or axial loading shorted out. Solid symbols indicate data from the ballasted deck structures.

6.1 Girder Spans

Measured static stresses in girder bottom flanges are plotted against the corresponding theoretical static stresses in Figure 1. The Alpha factor varied between 0.34 and 1.11. It is clear from the data that an Alpha factor of 0.85 as specified in the A.R.E.A. Manual is too low, and that an Alpha of 1.0 is a more appropriate assumption to make in evaluating most physically untested railway bridge girders. The two occurrences of an Alpha factor in excess of 1.0 came from two simple Deck Plate Girder spans. Figure 1 shows the advantage of bridge testing for most cases.

Figure 2 shows the same work trains with full impact (dynamic factor). The ratio of measured dynamic stresses to theoretical dynamic is less than 1.0 in all the recorded cases. Clearly, the impact formula specified in the A.R.E.A. Manual, originally derived for a rare event [3], is not appropriate for fatigue calculations.

Figure 3 is a modified version of Figure 2, with impact reduced to 10% of the A.R.E.A. value. Based on this data, one can conclude that for fatigue evaluation, it is quite safe to use an impact factor equal to 10% of the A.R.E.A. impact value, under certain operating conditions.

6.2 Stringers

As seen in Figure 4, the Alpha factor for stringer bottom flanges ranged from 0.32 to 1.35, and was generally less than 1.0, except for a few cases. In those few cases, the floor system had multiple stringers per rail. One stringer would record high stresses, while the adjacent ones would record low stresses. The uneven distribution of loads is due to small differences in elevation that prevent the ties from resting properly on some of the stringers. Again the Alpha factor needs to be 1.0, and not 0.85 or 0.8 (A.R.E.A. values for spans less than and greater than 23 meters respectively).

Figure 5 clearly illustrates that the ratio of measured dynamic stresses to theoretical stresses (including full theoretical impact) is less than 1.0.

Figure 6 shows that for fatigue life evaluation, it is safe to use a reduced impact factor equal to 25% of the theoretical impact specified in the A.R.E.A. Manual.

6.3 Truss Spans Bottom Chords

Figure 7 shows static stresses measured in the of bottom chords of the truss spans plotted against corresponding theoretical stresses. Except for one case, all the measured stresses were lower than the theoretical stresses. The Alpha factor varied from 0.42 to 1.0. The exception was a double track pin connected "fish belly" deck truss. The Alpha factor of 0.70 as specified in the A.R.E.A.



Manual is too liberal. A value of 0.95 might be more appropriate. However, it is our opinion that an Alpha factor of 1.0 should be used.

Figure 8 shows that, as in the earlier cases, the ratio of measured dynamic stresses to theoretical stresses (including full theoretical impact) is less than 1.0.

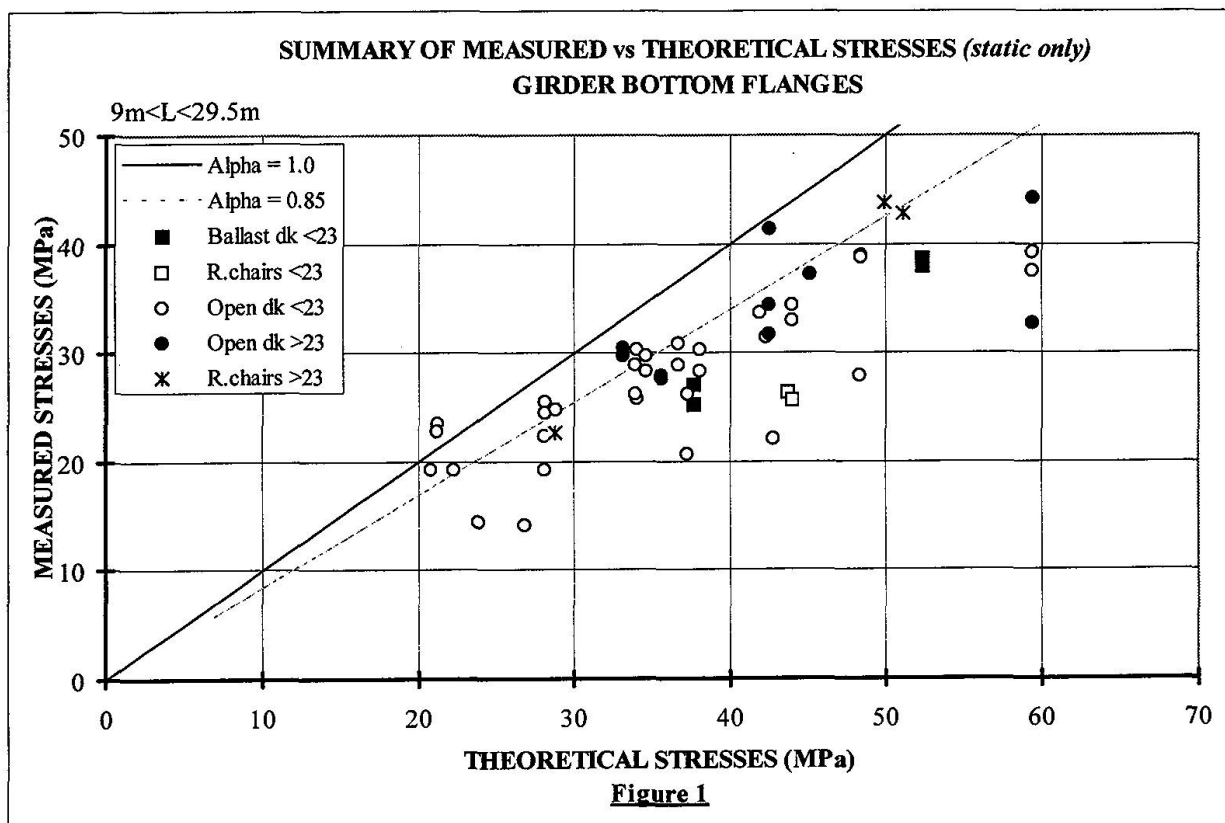
Figure 9 shows that even with no impact applied to the theoretical stresses, the measured dynamic stresses are still less than the theoretical stresses (with 1 exception). Our recommendation would be to use some nominal value for the theoretical impact (say equal to 10% of the A.R.E.A. value).

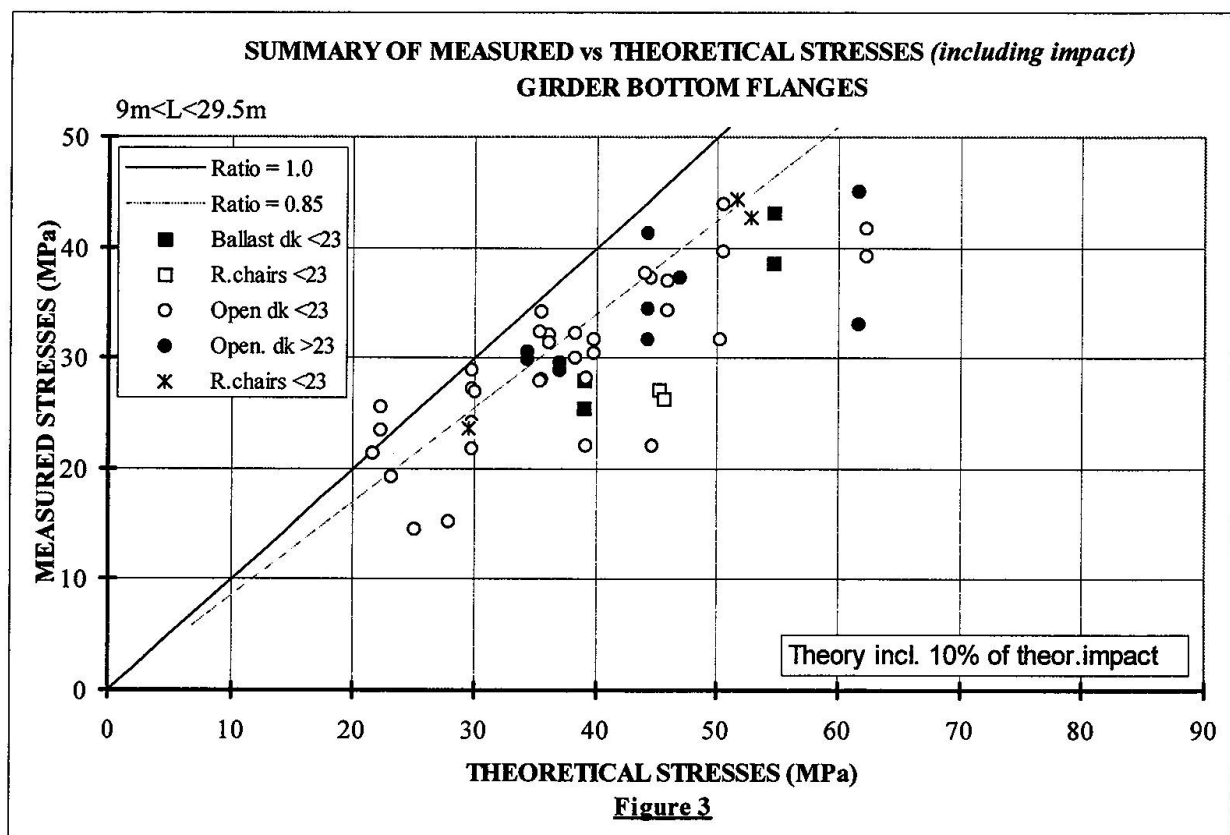
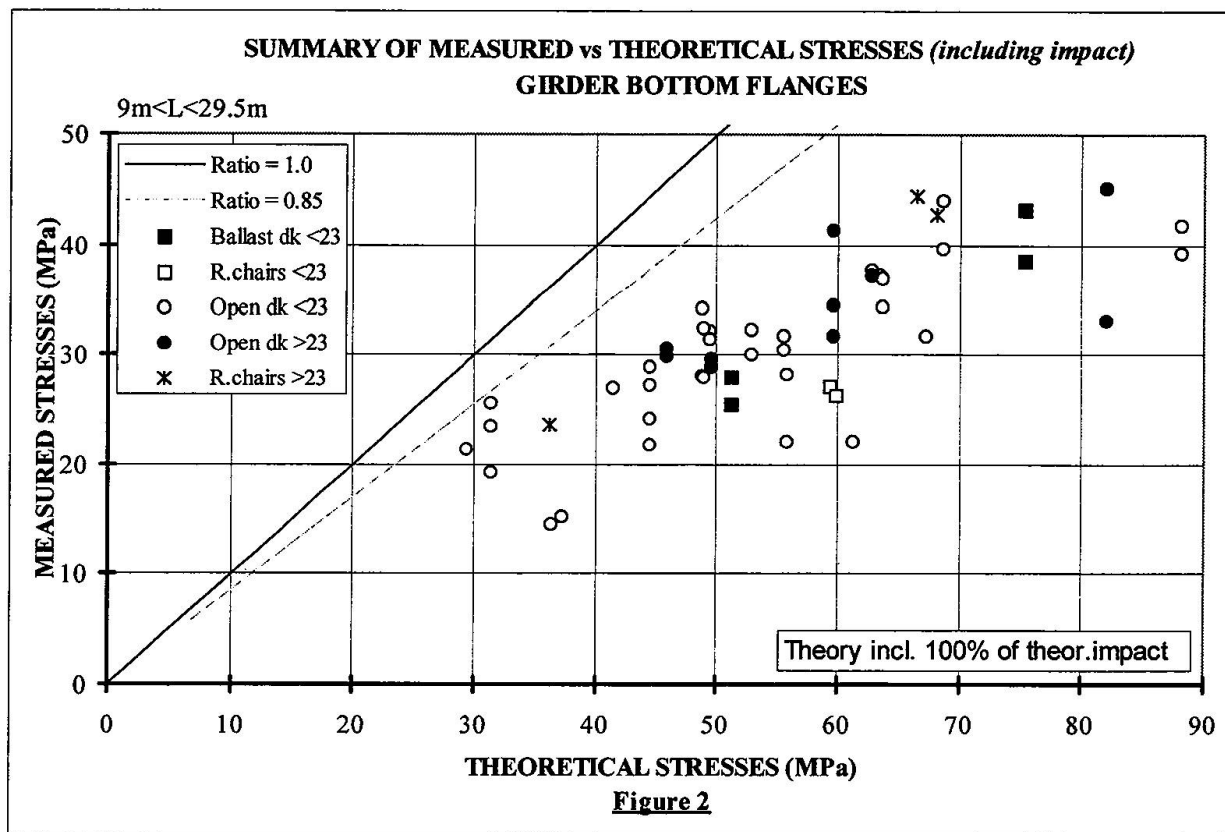
7. Concluding remarks

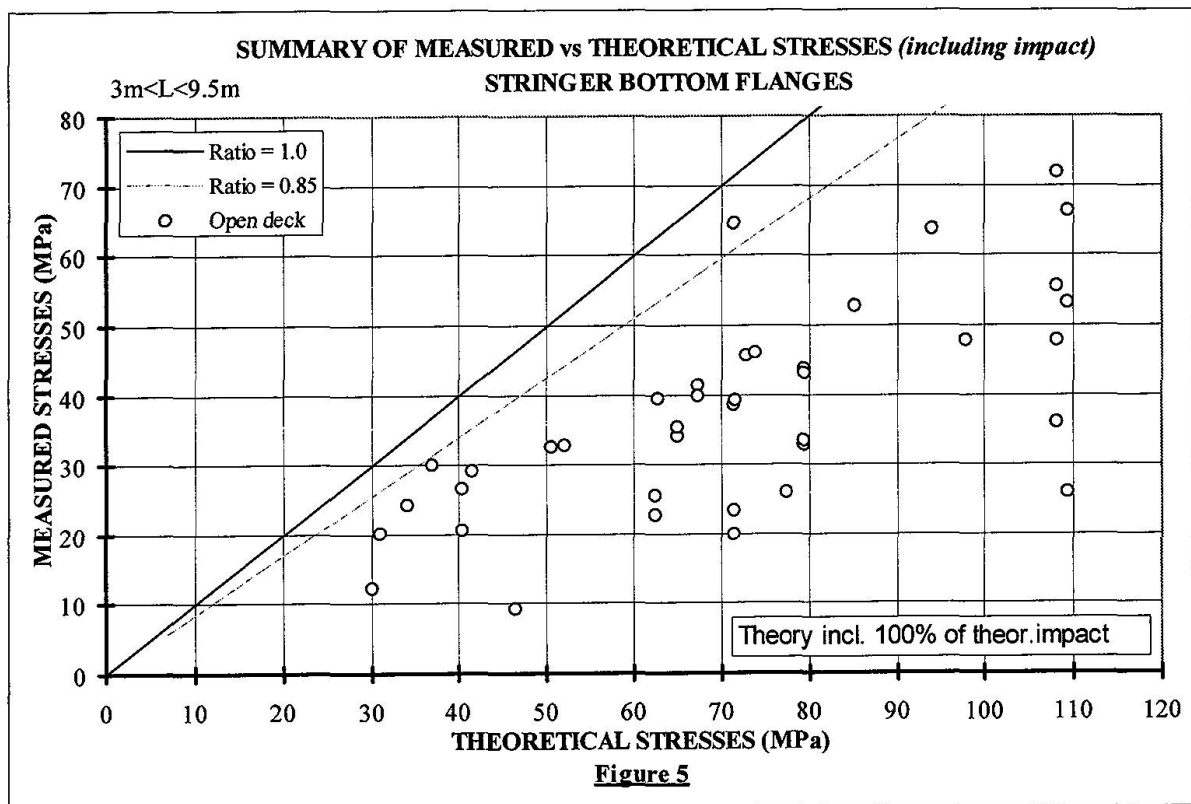
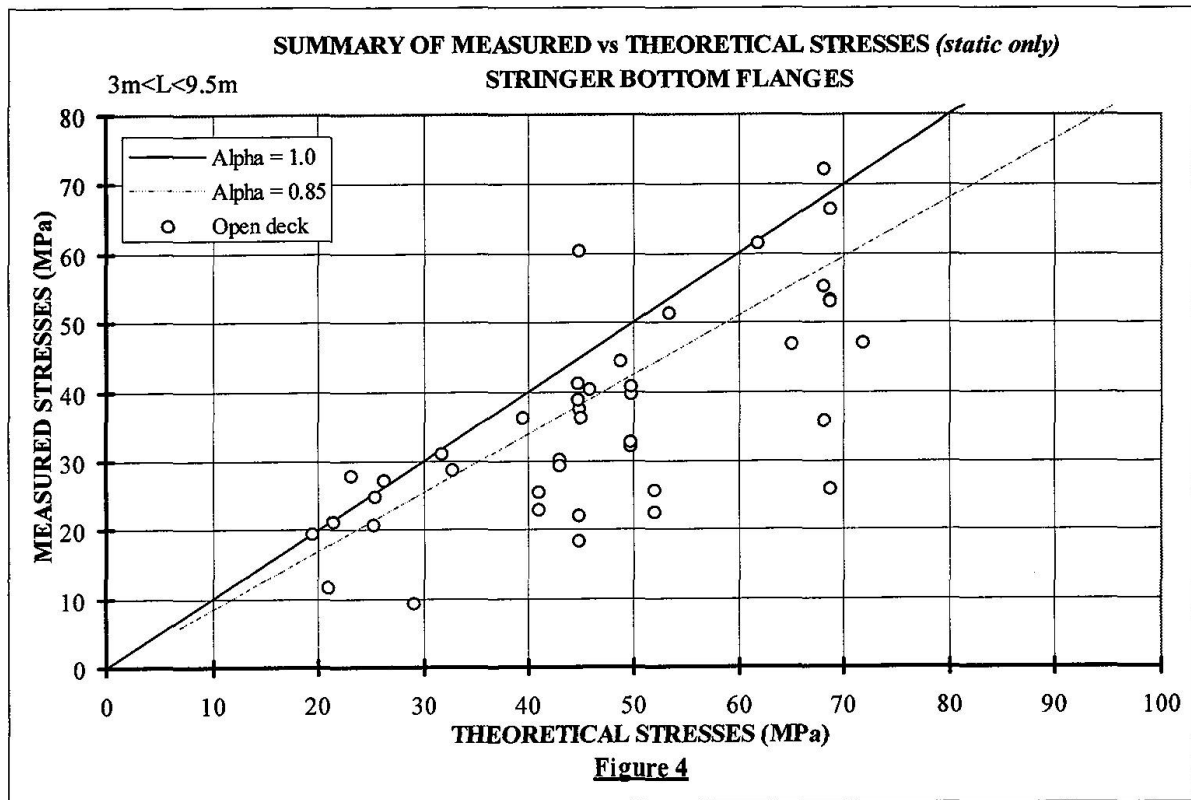
Measured static stresses and impacts outlined in this paper are generally lower than stresses calculated using conventional analytical techniques. In some cases remedial measures can be delayed for long periods of time. In overstressed member, testing will often point the way to less expensive retrofits, repairs or strengthening. In the majority of cases, bridge testing saves money.

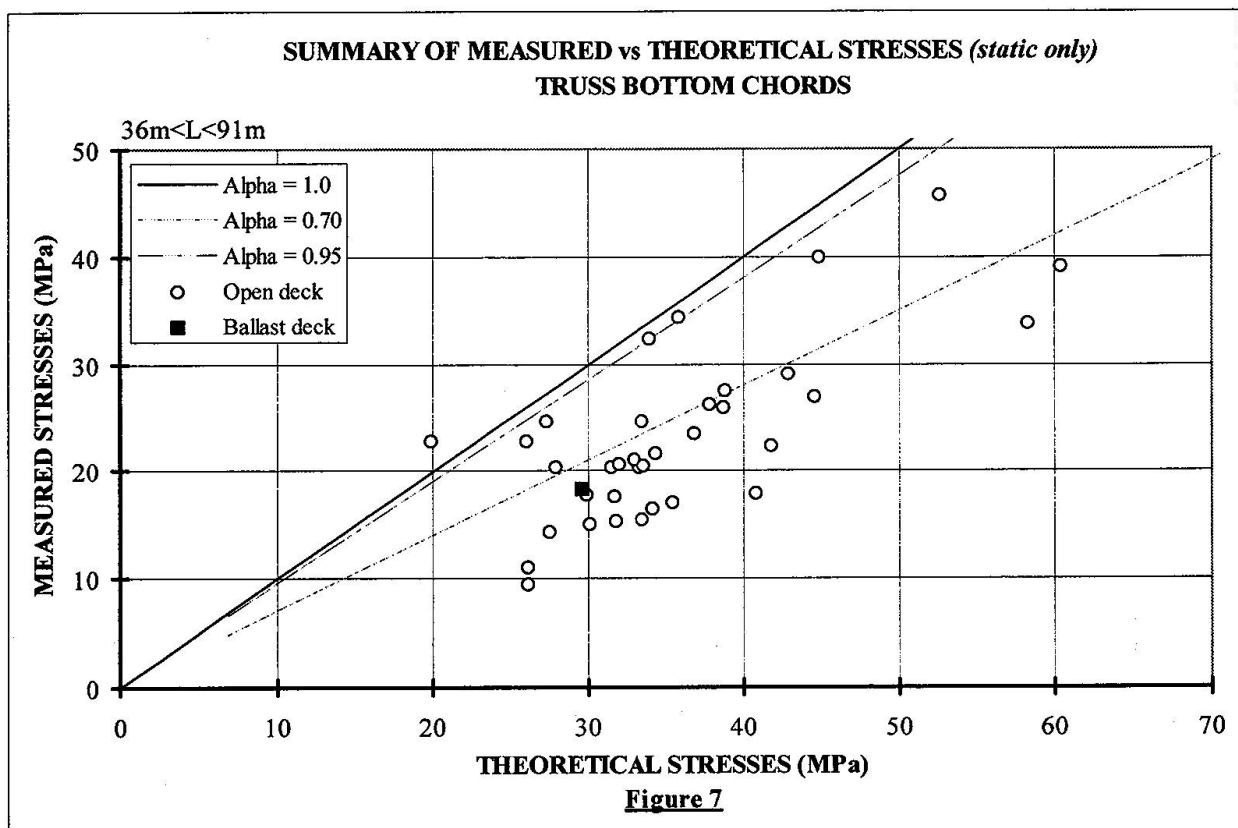
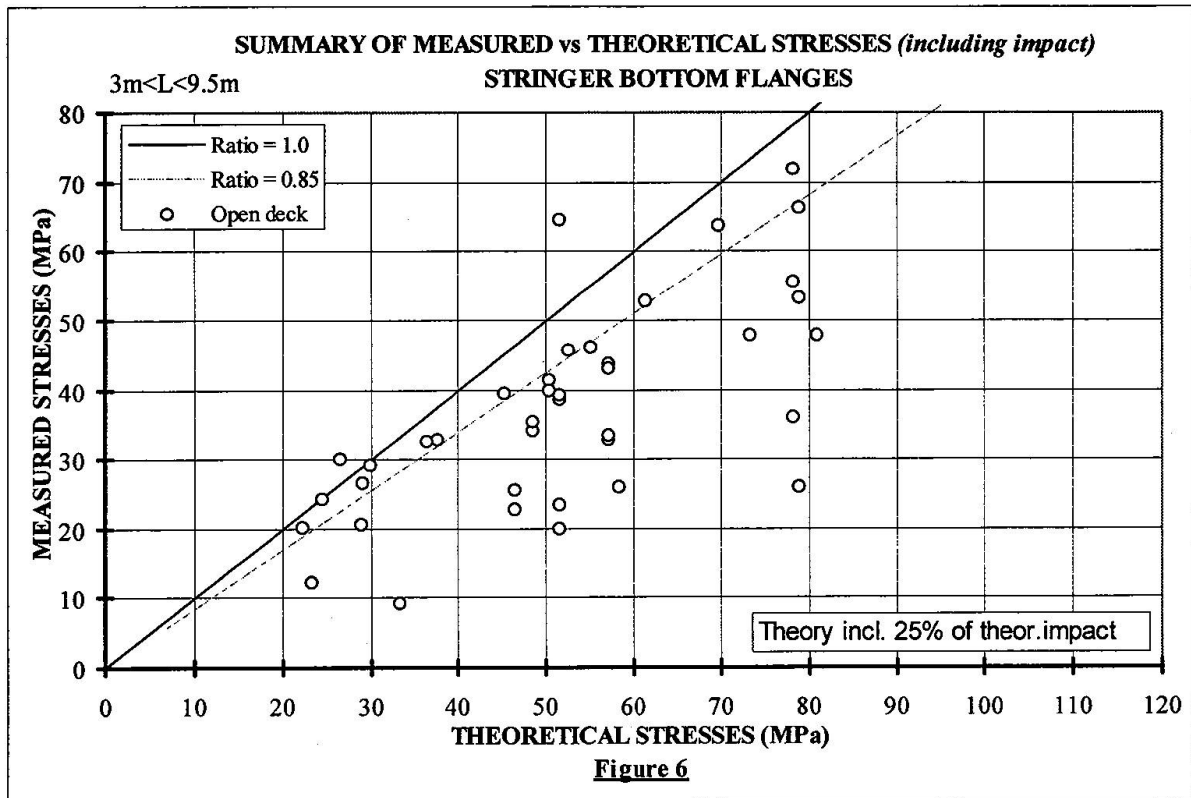
Nevertheless, since the test data shows that there are many exceptions, it is not recommended to blindly assume that such is always the case. *A reasonable upper bound for static data on the three classes of members reviewed in this paper requires an Alpha factor of 1.0.* Without some field testing it is not appropriate to assume a lower value.

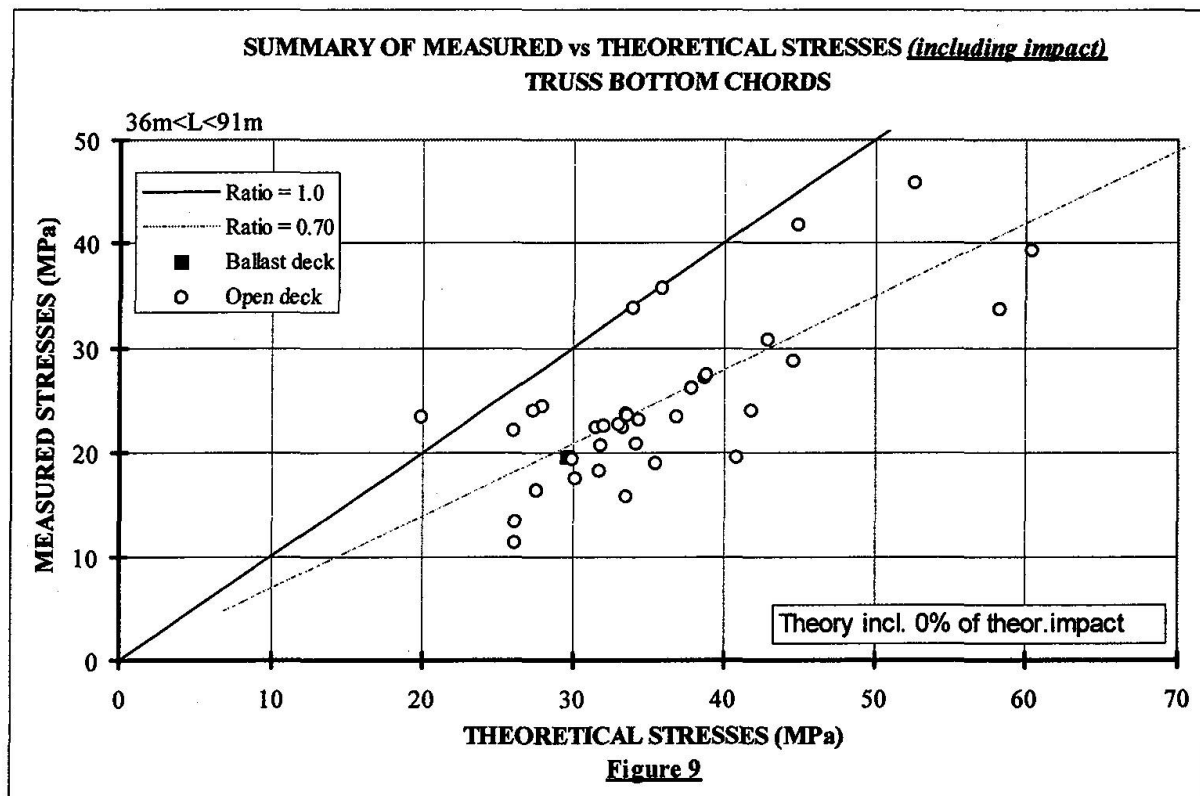
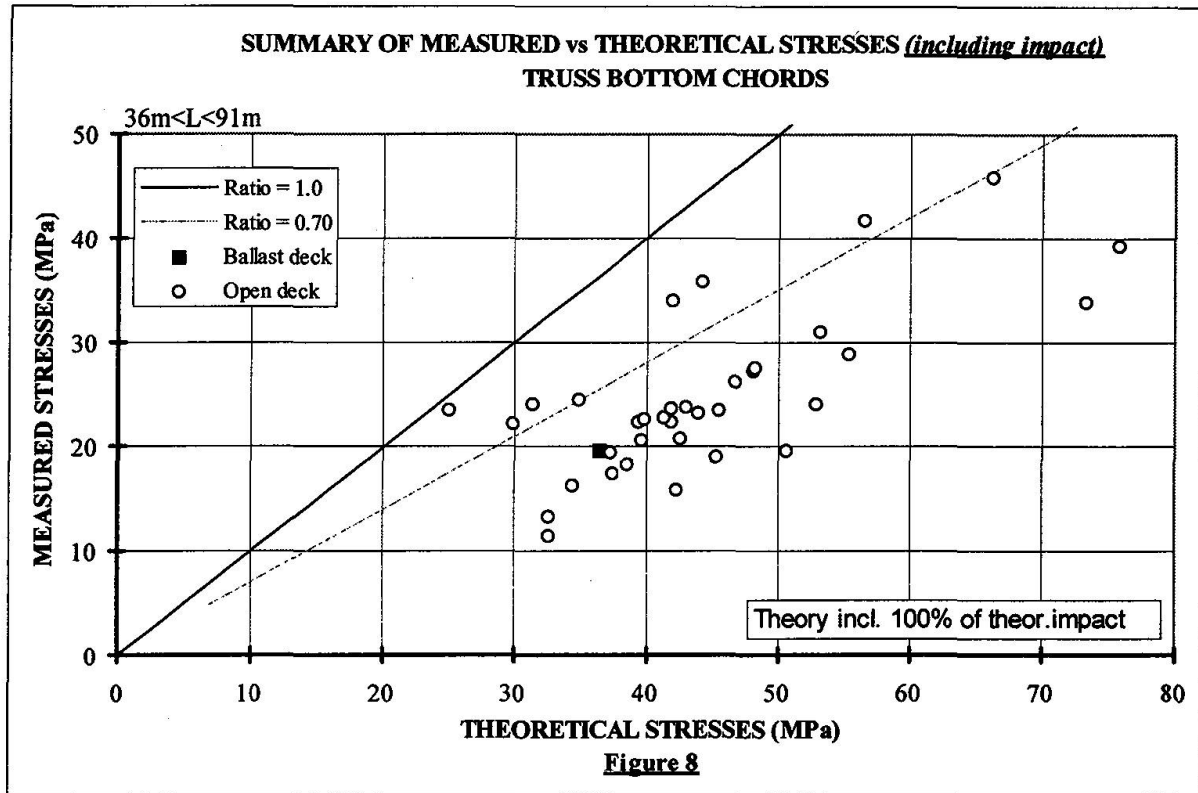
Impact factors originally designed to cover occasional occurrences during the life of a structure are much too conservative. The test data indicates that for fatigue evaluation purposes, impact factors lower than those specified in the A.R.E.A. Manual can be used. Our recommendation for appropriate impact values are: 10% of the A.R.E.A. value for girder bottom flanges, 25% of the A.R.E.A. value for stringer bottom flanges, and 10% of the A.R.E.A. value for truss bottom chords.











Acknowledgments

The authors wish to thank Romel Scorteanu, Project Engineer, who was responsible for the data acquisition, for his contribution, present and former members of the Rating and Testing groups at CN, and R.W. Richardson, Chief Engineer, for his continued support.

Disclaimer

The data provided in this report is of a highly technical nature and greatly summarized. Readers need to be extremely cautious in its use.

References

1. SWEENEY, ROBERT A.P., OOMMEN, GEORGE, and LE, HOAT, A Summary of Seven Years of Railway Bridge Testing at Canadian National Railway, Bulletin of the A.R.E.A. #756, May 1996, pp 333-347.
2. American Railway Engineering Association Manual of Recommended Practice, Chapter 15, Steel Bridges, Current to 1995.
3. BYERS, WILLIAM G., Impact from Railway Loading on Steel Girder Spans, ASCE, N.Y. J.of Struct., June 1970, pp 1093- 1103.

Leere Seite
Blank page
Page vide

Stress Measurement and Repair of a Fatigue Cracked Box Girder Bridge

Kentaro YAMADA
Professor
Dept. of Civil Eng.
Nagoya University
Nagoya, Japan

Tatsuya OJIO
Graduate Student
Dept. of Civil Eng.
Nagoya University
Nagoya, Japan

Shigenobu KAINUMA
Research Associate
Dept. of Civil Eng.
Nagoya University
Nagoya, Japan

Toshiyuki OBATA
Chief Engineer
Nat. Highway Office
Min. of Construction
Nagoya, Japan

Summary

A three span continuous box girder bridge in Nagoya was subjected to very heavy traffic, amounting to over 55,000 vehicles per day on three lanes and with about 50 percent trucks. In 1988 fatigue cracks were observed at diaphragm corners after 20 years of service. The fatigue damaged diaphragm corners were repaired by high strength bolted splices. Truss members were also added to stiffen the diaphragms and the cross beams. In the summer and the fall of 1996 stress measurements were carried out to investigate a method for measuring truck axle weights and to carry out a fatigue assessment of the orthotropic steel decks and diaphragm corners. In this paper the case history of the box girder bridge is summarized and the preliminary results of stress measurement are presented.

1. Introduction

Severe deterioration in highway bridges, such as deterioration in concrete decks and fatigue cracks in steel members, became noticeable to bridge engineers in the 1980s. This led to various research projects on repairing and retrofitting of aged and deteriorated highway bridges in Japan. Various case studies were carried out when severe deterioration was found in particular bridges.

This paper describes a case history of a three span continuous box girder bridge which exhibited fatigue cracks at diaphragm corners in 1988. The bridge was subjected to some of the heaviest loads in Japan. The stress measurement described here was carried out in 1996 as a part of the investigation to re-evaluate the effectiveness of the past rehabilitation measures, and to estimate wheel loads of trucks in service, which is essential for fatigue assessment of the bridge. The estimation of the wheel loads was carried out using the measured stresses at longitudinal ribs in the orthotropic steel deck.

2. Bridge description

2.1 History of the bridge

The three span continuous box girder bridge was constructed in 1964 with spans of 77 m, 96 m and 77 m. It is situated near a large port, and is subjected to very heavy traffic, since only a few alternative routes are available nearby. The bridge carries 3 traffic lanes in each direction on its orthotropic steel deck, as shown in Figure 1. Average daily traffic was about 55,000 in one direction in 1994, and about 43 percent of vehicles were trucks. Some of these were believed to be overloaded.

After about 25 years in service, fatigue cracks were found at corners of diaphragms and at sole plates of supports. A committee (Chairman; Prof. Nishino) was formed to investigate the extent of the damage, causes of the cracks and ways to retrofit the bridge. Intensive investigations, such as stress and vibration measurements and structural analysis by the finite element method, were carried out to find the best possible ways to retrofit the bridge. Based on such investigations the cracked parts were strengthened by high strength bolted splices, and truss members were added

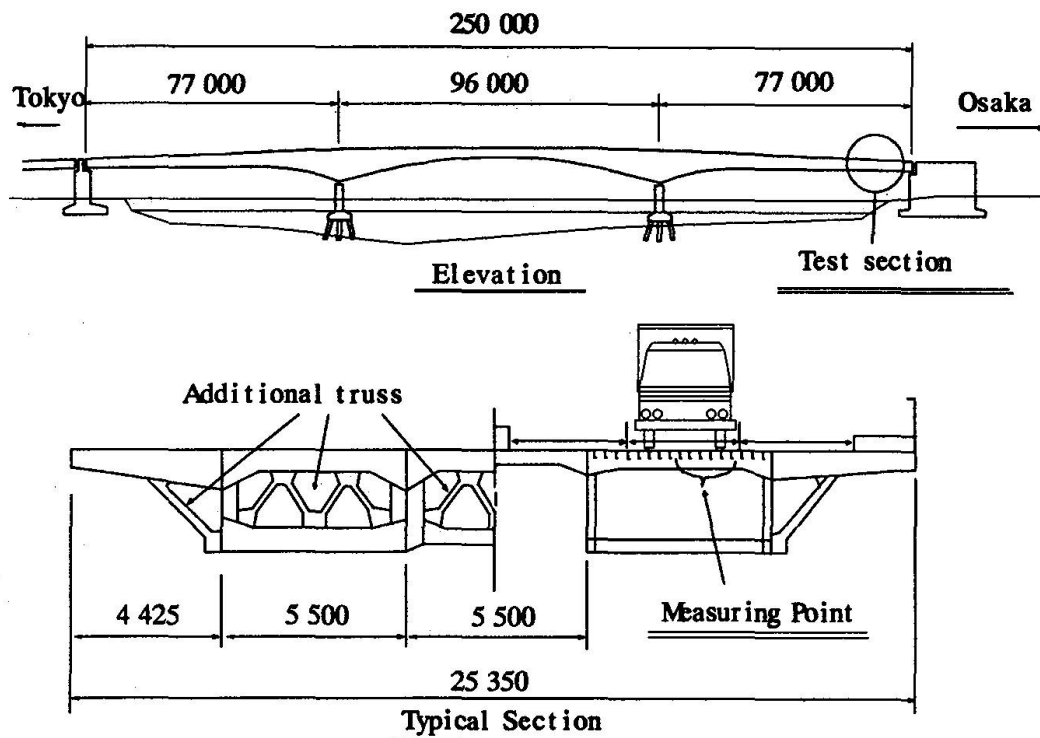


Fig. 1 Orthotropic steel deck bridge

to stiffen all diaphragms and every other cross ribs. The rehabilitation scheme seemed successful, and no further fatigue damages were observed at these stiffened parts. However, recent inspection revealed that a few additional cracks were found at the diaphragm corners which were not retrofitted eight years ago, because no fatigue cracks were observed at that time.

A study group (Chairman; Prof. Yamada) was formed to evaluate the effectiveness of the previous retrofitting, ways to retrofit the additional cracks, and overall resistance of the bridge against fatigue. The work is still underway. The stress measurements and estimation of the wheel loads described here is the part of the investigation.

2.2 Orthotropic steel deck with open ribs

The orthotropic steel deck of the box girder bridge is schematically shown in Figure 2. It has a 12 mm thick deck plate, stiffened longitudinally at every 300 mm with bulb plates (open ribs) of 180 mm wide and 9.5 mm thick. About 80 mm thick asphalt pavement is placed over the deck plate. Diaphragms are placed at every 7.7 m with four cross beams of which are 1.54 m apart between the diaphragms. As mentioned previously, the truss members were added to all diaphragms and every other cross ribs in order to stiffen them in 1988/89 retrofitting.

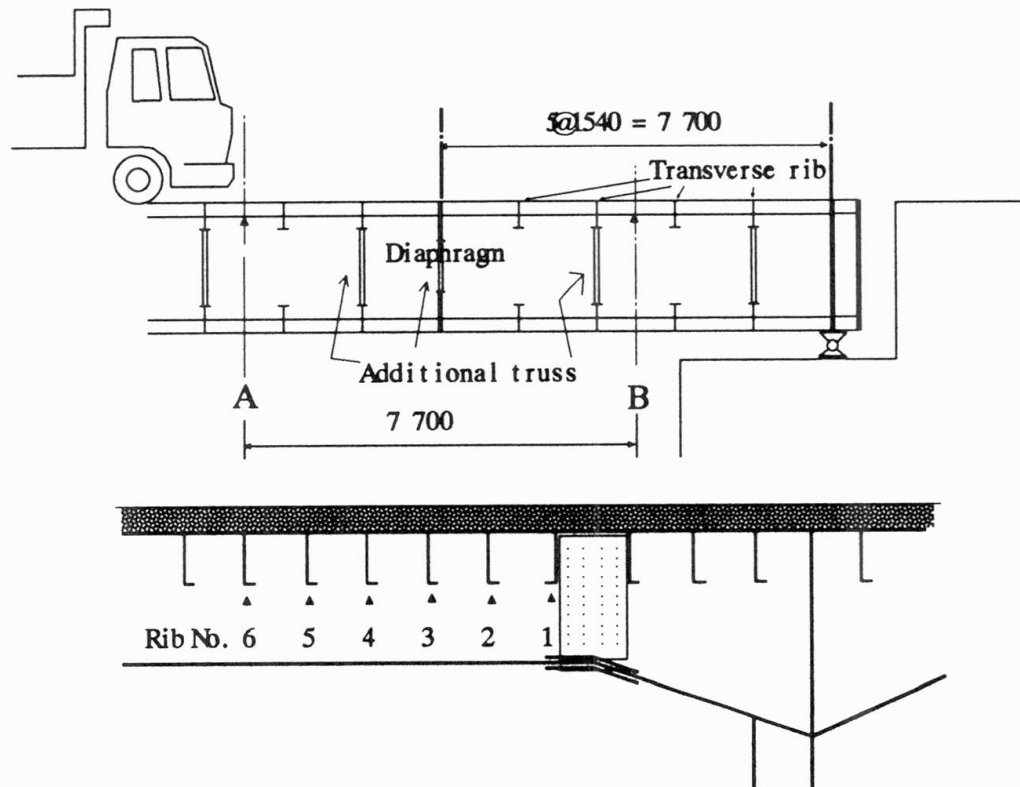


Fig. 2 Orthotropic steel deck of test bridge

3. Estimation of wheel loads

3.1 Procedure of wheel load estimation

Since the open ribs of the orthotropic steel deck are rather flexible, strain recordings measured at the open ribs can be used to estimate the wheel loads passing on them

The procedure used in this investigation is as follows;

- FEM analysis** : The finite element analysis was carried out for the orthotropic steel deck of interest to determine influence surfaces for all locations of strain gages, that were placed at the mid-span of the longitudinal ribs.
- Effect of tire loading** : Wheels with single tire and double tires with an unit weight were placed at different positions to calculate stress waves of the longitudinal ribs. Loading areas of the tires were determined according to JRA Specifications. Through such analysis it was determined to use six strain gages at two sections, A and B, near the supports, which were 7.7 m apart, as shown in Figure 2.
- Strain measurements** : Strain histories were recorded dynamically using Digital Data Recorder, and the data was transferred to a personal computer for further analyses. Typical strain recordings for 2-axle truck and 3-axle truck are shown in Figure 3.

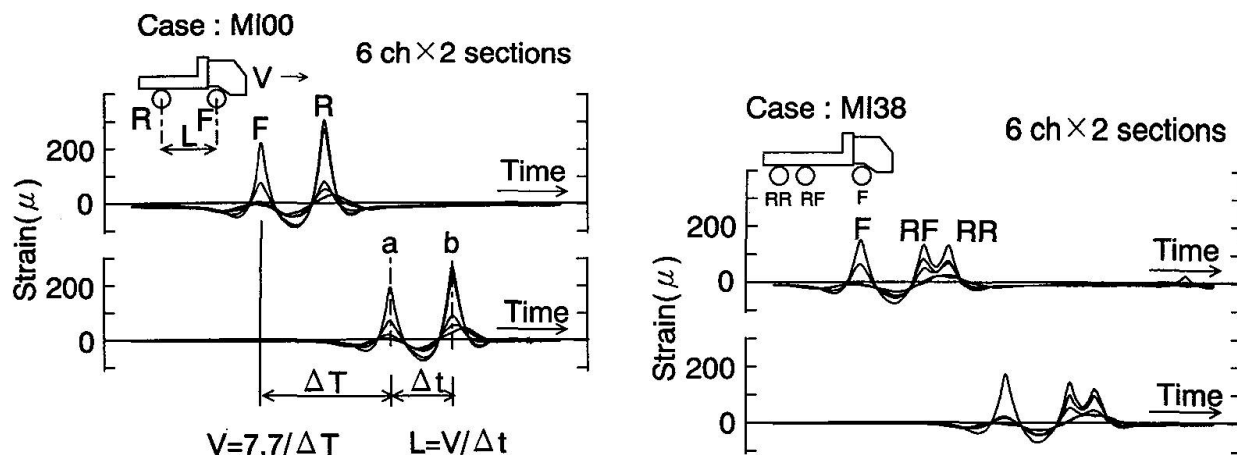


Fig. 3 Strain histories due to running of test trucks

d) **Tire types and their positions** : From six strain recordings peak strains corresponding to wheels passing on the mid-span of the ribs were determined first. Then, three largest strain recordings were picked up, and tire position was determined. Single or double tires was also clarified from the shape of the strain waves, as shown in Figure 4.

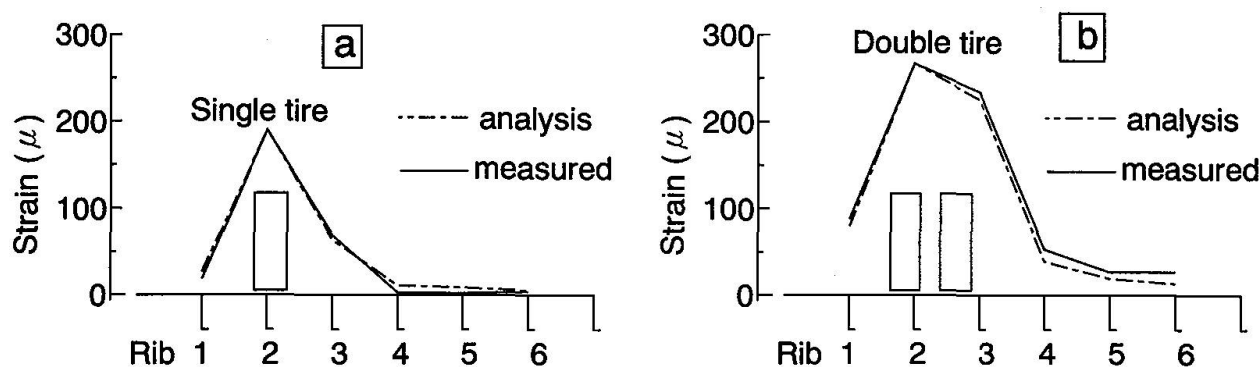


Fig. 4 Stress distribution of six ribs at a and b

e) **Wheel weight and number of axles** : The weight of each wheel was determined by comparing measured strains with the computed strains for an unit wheel load. Number of axles of each truck was also determined by checking distance between the wheels. These process was carried out in a personal computer, and they are visually monitored through CRT screen.

f) The velocity of the trucks was also determined from the time needed for the front wheel to pass the two test sections.

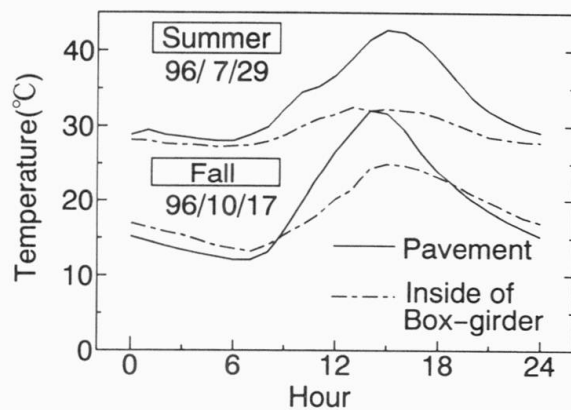
3.2 Stress Measurements

Stress measurements were carried out in the summer (July) and in the fall (October) of 1996. Strain gages to measure wheel loads were attached at the lower edge of six longitudinal ribs at two sections, A and B. Two test trucks were used in the summer experiments for calibration of this procedure. Dynamic strain were recorded digitally for 10 seconds for the summer experiments, when the test trucks passed on the test sections. About 45 trucks of various types were also measured. Accidentally, some other trucks were also recorded in the 10 second recordings, and total of 430 axles were recorded.

For the fall experiment strain recordings were automatically recorded for 2.5 seconds, whenever any strain in the section A exceeded 50 micro-strains. The measurement was carried out for 30 minutes in ever hour for 24 hours. About 200 trucks were monitored in this way in 30 minutes. The data was then transferred to an personal computer, which needed for 15 to 20 minutes. About 5,000 trucks were recorded for 12-hour recording.

4 Summer experiment (July 1996)

4.1 Measurement for test trucks



The first measurement was carried out in the end of July, 1996. It was the mid-summer in Nagoya and the temperature at the bottom of the asphalt pavement of the orthotropic deck was between 27 and 49, as shown in Figure 5. Two test trucks were used, as shown in Table 1. They were a 2-axle dump truck of 220 kN gross vehicle weight (GVW), and a 3-axle dump truck of 223 kN GVW. Drivers of the test trucks were asked to drive the trucks intentionally in the left, the center and the right sides of the mid-lane at different velocity. The test trucks ran with speed between 22 and 58 km/h over the test sections.

Fig. 5 Temperature of asphalt pavement

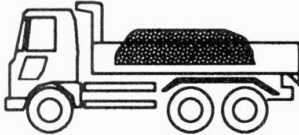

| Type |  | | |  | |
|------------|--|------|------|---|------|
| | F | RF | RR | F | R |
| | Wheel load (kN) | | | | |
| | F | RF | RR | F | R |
| 96 'Summer | 27.8 | 43.7 | 39.4 | 35.0 | 74.6 |
| | GVW=223 kN | | | GVW=220 kN | |
| 96 'Fall | 25.9 | 39.9 | 33.8 | | |
| | GVW=199 kN | | | | |

Table 1 Wheel loads of test trucks

From the recorded strains the wheel loads were estimated. The estimated wheel loads, W_e , are plotted against actual wheel loads, W_a , measured statically at a weigh station in Figure 6. It was found that W_e for the front and rear wheels were about 20 percent higher in average than W_a . The scatter of the estimated wheel loads was also observed owing to the scatter in the measured strain recording, which probably came from the vibration of the truck during the passage over the test sections.

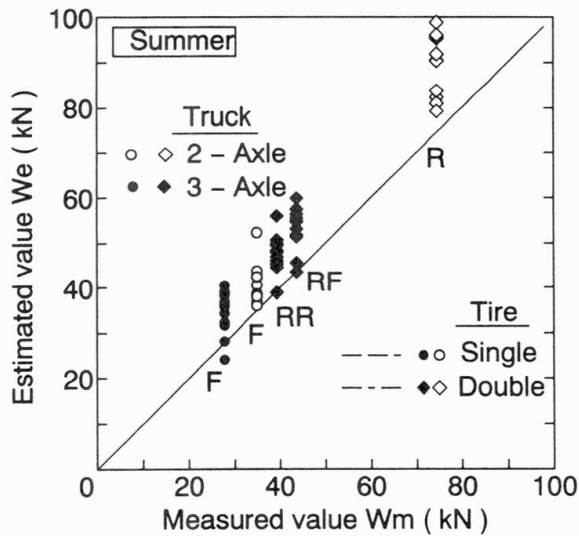


Fig. 6 Comparison of measured and estimated wheel loads of test trucks

4.2 Measurement for trucks in service

The wheel loads of the passing trucks of various types were also estimated. The result is plotted in Figure 7. The wheel loads of these trucks were not known, but the estimated wheel loads for the front wheel (single tire) are ranging from 4.9 kN to 64 kN. The maximum wheel loads showed scatter from 4.9 kN to 98 kN. The legal limit of the wheel loads was 49 kN in Japan. From the measured strain the wheel positions were also determined through the analysis and plotted in Figure 8. For 312 wheel loads heavier than 4.9 kN the wheel positions were between the ribs 1 and 5, which were 1.2 m apart. The majority of the wheels passed between the ribs 2 and 3.

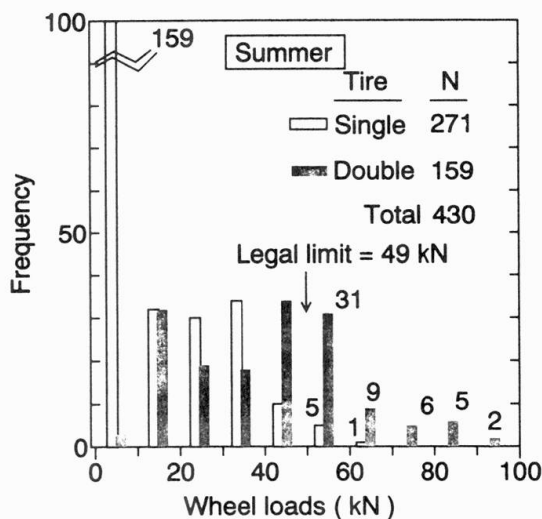


Fig. 7 Frequency of estimated wheel load position

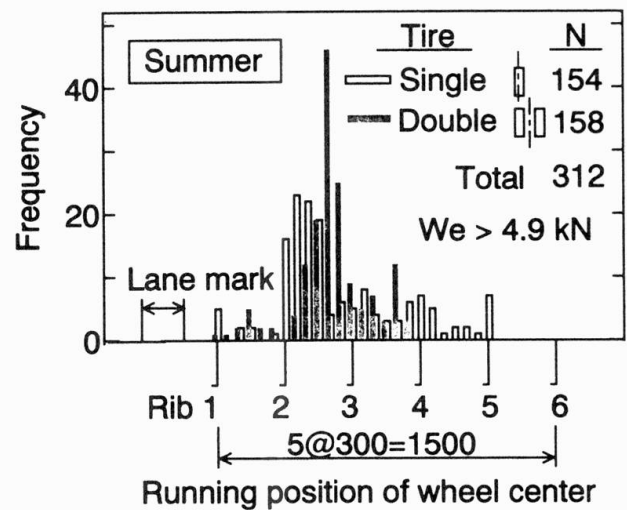


Fig. 8 Frequency of estimated wheel position

5 Fall experiment (October 1996)

5.1 Measurement for test truck

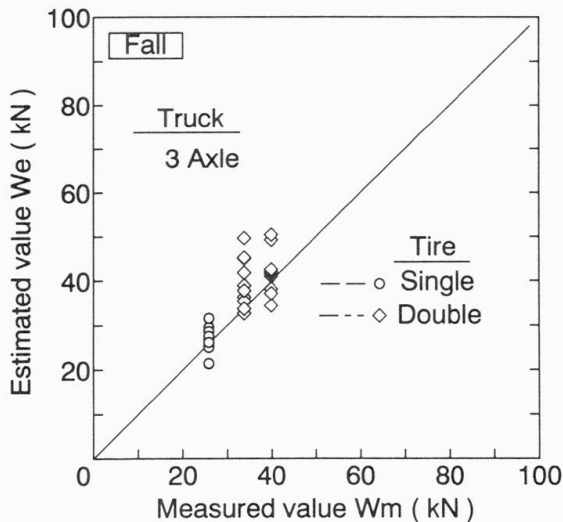


Fig. 9 The comparison of measured and estimates wheel loads of test trucks

The measurement was once more carried out in the mid-October, 1996, when the temperature of the asphalt pavement was ranging between 12 and 32, as shown in Figure 5. A 3-axle truck of 199 kN, which ran over the test sections 12 times, was used to calibrate the results. The wheel loads of the test trucks were estimated using the same technique used in the summer experiments. The results are plotted in Figure 9. The average estimated wheel loads were about 5 percent more than the actual wheel loads

The difference in the ratio of the average estimated wheel loads to the statically measured ones between the summer and the fall experiments was about 15 points. In this period supports near the section B was temporarily jacked up for replacement works from metal shoes to rubber ones. The effect of such change in structural details on the test results is unknown at this moment. The increase in the stiffness of the asphalt pavement above the orthotropic deck may also attribute to the

difference. The temperature of the asphalt pavement dropped by about 15 when the fall experiment was carried out. Increase in the stiffness of the asphalt pavement results less strain in the longitudinal ribs, and hence less estimated wheel load than that of the summer experiment.

5.2 24-hour measurement for trucks in service

The most of the recorded strain waves were automatically analyzed by a personal computers. About 10 percent of recorded strain waves were analyzed by inputting velocity of the trucks, since it was not computed automatically in the wave analysis. About 13,000 wheel loads were estimated for total 12 hours recordings.

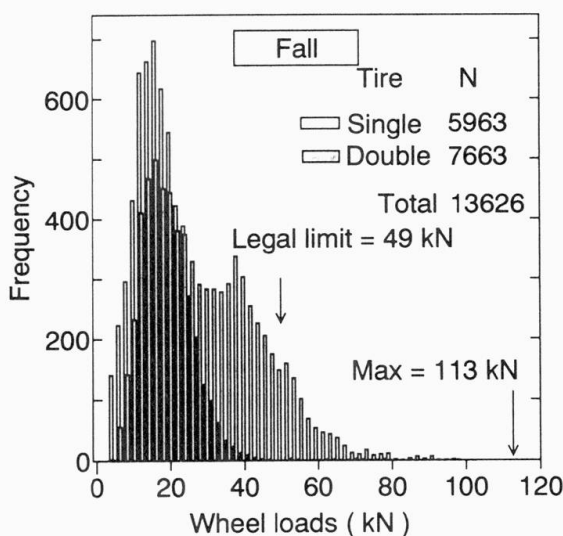


Fig. 10 Frequency of estimated wheel load

The estimated wheel loads, We , are summarized in Figure 10. Note that these wheel loads are for the trucks in which one of the strain recordings exceeded the trigger level of 50 micro-strain. The maximum wheel load observed during the 12-hr measurement was 113 kN. The frequency distribution of wheels with double tires shows two peaks, one around 39 kN, and the other at about 15 kN. The latter seemed the wheel loads when the truck were not loaded.

The running position of all wheels are plotted in Figure 11. The majority of the wheels passed between ribs 2 and 3, and some passed between ribs 3 and 4. In these areas ruts were observed, and the trucks seemed to run along such ruts.

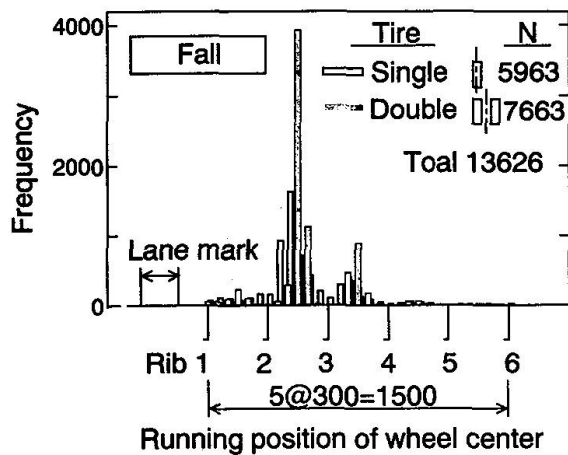


Fig. 11 Frequency of estimated wheel position

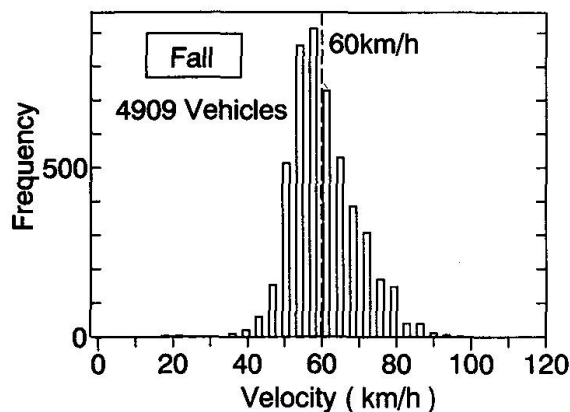


Fig.12 Frequency of vehicle velocity

The velocity of each truck in service was also computed. The distribution of the velocity is plotted in Figure 12. The average speed was about 57 km/h. Approximately 50 percent of the trucks ran with speeds over 60 km/h, while speed limit of this road was 60 km/h.

Once the speed of each truck was known, one can compute the wheel spacing. The distribution of the computed wheel spacing is shown in Figure 13. There are several groups of wheel spacing. Compared with the configuration of the trucks currently used in Japan, the wheel spacing seems to correspond to (a) tandem wheels (about 1.3 m), (b) main spacing of dump trucks or tractors, (c) main spacing of 3-axle trucks or short trailer trucks, and (d) main spacing of long trailer trucks.

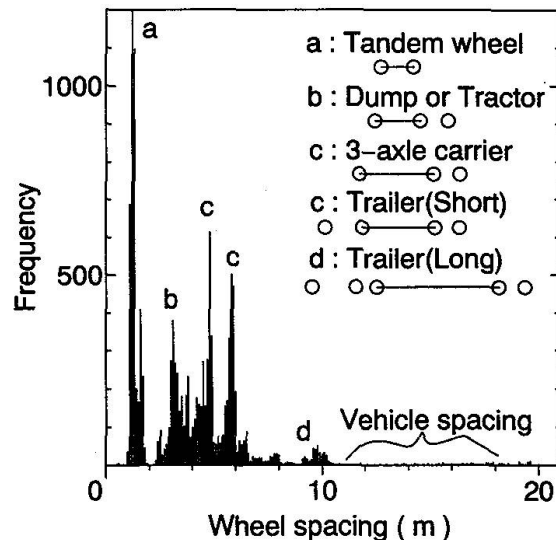


Fig.13 Frequency of estimated wheel spacing

6 Summary of findings

Some fatigue damages were observed in 1988 in a three span continuous box girder bridge situating in the heavily loaded highway . They were retrofitted by applying high strength bolted splices to the cracked parts, and adding truss members in diaphragms and cross ribs to stiffen the box section. The study is currently underway to investigate the overall durability of the bridge against fatigue. The stress measurements and the estimation of wheel loads described here were one part of the investigation. The followings summarize the findings of the stress measurement and the estimation of the wheel loads using the strain history recorded dynamically in the longitudinal ribs of the orthotropic steel deck.

- 1) The procedure used in this study to estimate the wheel loads in service seems feasible. Relatively consistent values of estimated wheel loads were obtained for the wheel loads of the test trucks, of which the weight was measured statically at the weigh station.
- 2) The effect of the temperature of the asphalt pavement on the deck plate affect the estimated wheel loads of the test trucks. In the summer experiments the estimated wheel loads were about 20 percent higher in average than the measured ones. In the fall experiment the estimated value was about 5 percent higher for all wheels. It was about 15 points less than the summer

experiment. The lower temperature may cause higher stiffness of the asphalt pavement, and hence less strains in the longitudinal ribs, which lead to less estimated wheel loads.

3) The position of wheels, the speed of vehicles and wheel spacing of trucks can be also computed from the strain recordings. The data may be used to define the type of trucks in service.

4) The digital dynamic recorder used in this study enable us to record the dynamic strain waves for 2.5 seconds, whenever the strain exceeded a certain value. It was possible to record strain wave for about 200 trucks in 30 minutes. The measurement was carried out automatically for 24 hours. This procedure opened a way to record strains only when the heavier wheel loads passed on the test section.

Acknowledgments

The authors are grateful to those who helped us in the summer and the fall experiments. They are those from No.3 Work Office of Nagoya Highway Work Office, the Ministry of Construction, those from Toyo Giken Consultants, especially Messrs. Shindo and Furuichi, those from Dept. of Civil Engineering, Nagoya University, and from Tokyo Sokki Kenkyujo.

References

1. MATSUI, S. and EL-HAKIM, A., Estimation of Axle Loads of Vehicles by Crack Opening of RC Slab, *Journal of Structural Engineering, JSCE*, 1989, pp.407-418. (In Japanese)
2. MOSES, F., Weigh-In-Motion System Using Instrumented Bridges, *Transportation Engineering, Proceedings of ASCE*, Vol.105, No. TE3, May 1979.
3. Hanshin Expressway, Committee on Hanshin Expressway Design Loads, Study on Design Loads of Hanshin Expressway, Technical Report, 1986. (In Japanese)
4. MIKI, C., MURAKOSHI, J., YONEDA, T. and YOSHIMURA, Y., Measurement of Vehicle Weight in Service, *Bridge and Foundation Engineering*, April 1987, pp.41-45. (In Japanese)

Leere Seite
Blank page
Page vide